

Preparation and Study of Thermal, Mechanical and Electrical Properties of Epoxy Based Composites Containing MWCNTs and PZT



By

Arif Ali

**Department of Chemistry
Quaid-i-Azam University
Islamabad, Pakistan
(2016)**

Preparation and Study of Thermal, Mechanical and Electrical Properties of Epoxy Based Composites Containing MWCNTs and PZT



A Dissertation submitted to the
Department of Chemistry, Quaid-i-Azam University Islamabad,
in the partial fulfilment of the requirements for the degree of

Master of Philosophy

In

Physical Chemistry

By

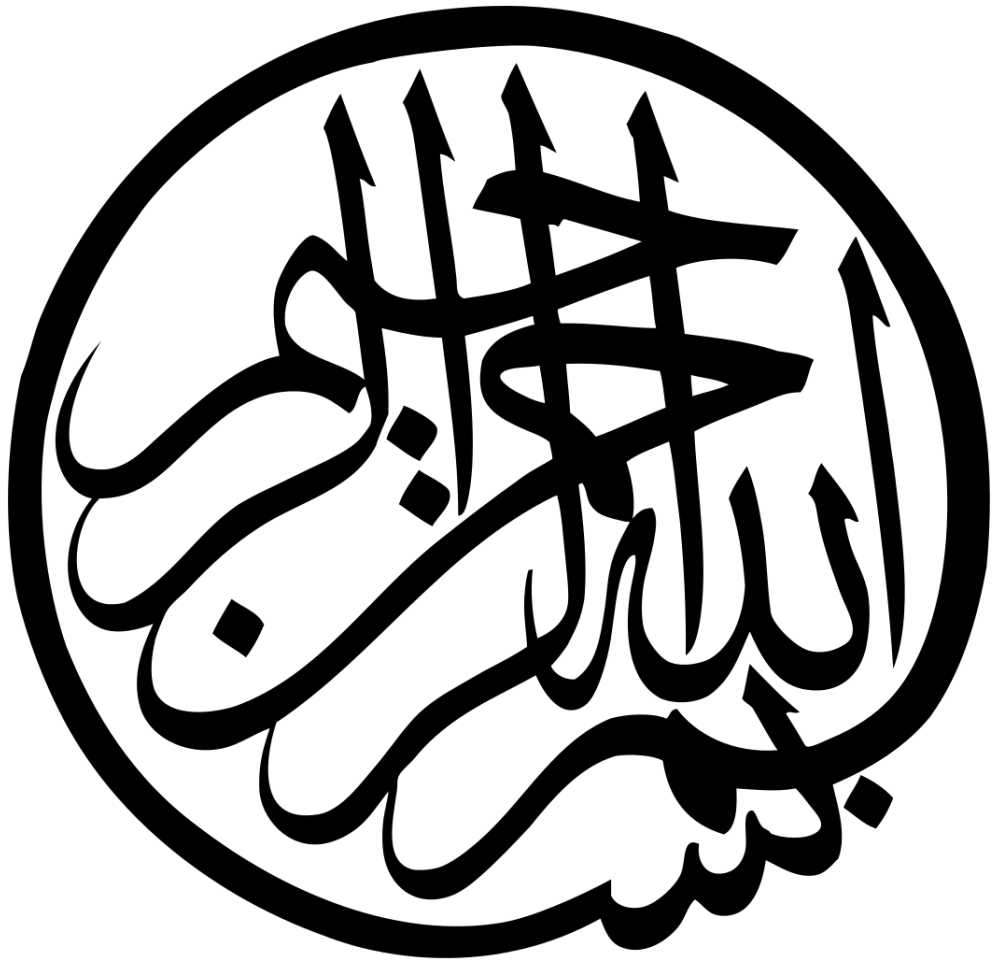
Arif Ali

Department of Chemistry

Quaid-i-Azam University

Islamabad, Pakistan

(2016)



DEDICATED
TO MY
LOVING PARENTS

Table of contents

ACKNOWLEDGEMENTS.....	iv
ABSTRACT.....	v
List of Figures.....	vi
List of Tables.....	viii
CHAPTER 1. INTRODUCTION	1
1.1 Composite materials	1
1.1.1 Matrix phase.....	1
1.1.2 Reinforcement phase.....	2
1.2 Polymer matrix composites	3
1.2.1 Thermosetting polymers as matrix material	3
1.2.2 Thermoplastic polymers.....	3
1.2.3 Applications of polymer matrix composites (PMCs)	4
1.3 Epoxy resin as matrix	4
1.3.1 Types of epoxy resins	5
1.4 Diglycidyl ether of Bisphenol-A (DGEBA)	5
1.4.1 Synthesis of DGEBA epoxy	6
1.4.2 Curing of epoxy	7
1.4.3 Cross linking Density	8
1.4.4 Curing agents	8
1.4.5 Curing reactions.....	9
1.4.6 Selection of curing agents.....	11
1.4.7 The stoichiometry.....	11

1.4.8	General properties of epoxy resin.....	12
1.5	Carbon nanotubes (CNTs) as reinforcement.....	13
1.5.1	Properties of CNTs	13
1.5.2	Applications of CNTS	14
1.5.3	Single walled carbon nanotubes (SWCNTs).....	14
1.5.4	Multiwalled carbon nanotubes (MWCNTs)	15
1.5.5	Epoxy containing MWCNTs	16
1.6	Piezoelectric materials	19
1.6.1	Piezoelectric materials and electromechanical properties	20
1.6.2	Piezoelectric composites	24
1.7	Present work.....	25
1.7.1	Strategies Developed.....	25
CHAPTER 2.	EXPERIMENTAL.....	27
2.1	Chemicals.....	27
2.2	Specifications of matrix and reinforcement used in the study	27
2.3	Specifications of Multiwalled Carbon nanotubes	28
2.4	Specifications of PZT	28
2.5	STEP 1	30
2.5.1	Purification of carbon nanotubes	30
2.6	STEP-2.....	31
2.6.1	Preparation of cured epoxy/MWCNT/PZT composite.....	31
2.7	Characterization of composites.....	32
CHAPTER 3.	RESULTS AND DISCUSSION.....	33
3.1	X-Ray Diffraction analysis(XRD).....	33
3.2	THERMAL ANALYSIS.....	35
3.2.1	Differential scanning calorimetry (DSC)	35
3.2.2	Thermogravimetric analysis (TGA)	41
3.2.3	Tensile testing	44

3.3	Electrical conductivity	60
3.4	Conclusions.....	62

Acknowledgement

Praise is to **Allah**, the Cherisher and Sustainer of the worlds, who showed His countless blessings upon us. Almighty Allah enabled me to compile my humble endeavors in the shape of this thesis. All respect goes to the **Holy Prophet Hazrat Muhammad (PBUH)** whose teachings strengthened our faith in Allah, who is the source of knowledge and wisdom for entire humanity, who clarified that pursuit of knowledge is a divine commandment.

I would like to extend my sincere gratitude to all those people who made this thesis possible. I am also heartily thankful to my dignified and respectable supervisor, **Prof. Dr. Muhammad Ishaq**, whose encouragement, supervision and support from the preliminary to the concluding level enabled me to develop an understanding of the subject. His expertise, valuable suggestions and patience, added considerably to my experience and enabled me to complete this research project.

I am especially grateful to my senior and lab fellow, **Dildar Ali Lakho** for his continuous guidance, without his participation it would not have been possible. It is a pleasure to thank all my lab fellows for their cooperation during my research work. The time spent in the company of these people has become a memorable part of my life.

The lively company of my friends specially **Azizullah Rajper** who relieved my moods in the times of tension and stress. I thank them for their pleasant company, unconditional support, love and care.

I am most indebted to my sweet mother, my brothers and my sisters for their endless prayers, matchless love and care. Words become meaningless when I have to say thanks to my parents and family; their prayers gave me strength and hope to accomplish this task and to pursue my goals.

Arif Ali

Abstract

Piezoelectric materials are widely used as sensors, transducers, medical diagnosis aerospace equipment, structural health monitoring and other energy harvesting devices, but the brittle nature of piezoelectric materials limits their operational strains, cycle life and ability to be integrated into complex shapes and structures while maintaining high sensitivity and reliability. Polymer matrix composites containing multi walled carbon nanotubes have attracted much attention due to their flexibility, ease of processing and improved mechanical properties. Carbon nanotubes are also responsible for the conductive nature of the epoxy-CNT composites due to good electrical properties. Above problems can be overcome by synthesizing piezoelectric composites having polymer matrix of good properties, conductive inclusions and piezoelectric material, these composites have improved mechanical and electrical properties than the single piezoelectric crystal. In this work piezoelectric composites are prepared which contains DGEBA (Diglycidal Ether of Bisphenol-A) as matrix, and 4,4'-Oxidianiline (ODA) as a curing agent for epoxy, multiwalled carbon nanotubes as conductive inclusions and lead zirconate titanate (PZT) as piezoelectric material. This work suggests that inclusion of MWCNTs enhances the piezoelectric properties by increasing the electrical conductivity of the composites, it also improves mechanical properties by decreasing brittleness of the material. This work seeks to understand how the weight % of the fillers i.e. MWCNTs and PZT effect the mechanical properties, the glass transition temperature, electrical conductivity and other parameters. Mechanical properties are determined by using tensile testing, different parameters were calculated e.g. toughness, young's modulus (modulus of elasticity), stress at break and ultimate tensile strength. Effect of fillers on glass transition temperature of epoxy matrix was studied by using differential scanning calorimetry (DSC), thermal degradation was studied by thermogravimetric analysis (TGA) which includes determination of different parameters e.g. maximum degradation temperature (T_{max}), temperature at which 10% degradation occurs (T_{10}) and char yield. Electrical conductivities of the composites were determined and effect of increasing the amount of fillers on the conductivities was studied.

List of figures

Figure 1.1: Epoxy ring	5
Figure 1.2: Structure of DGEBA epoxy.....	6
Figure 1.3: Synthesis of DGEBA epoxy.....	7
Figure 1.4: General reaction of epoxy curing.	10
Figure 1.5: General reaction of epoxy and amine.....	10
Figure 1.6: Three dimensional network of epoxy.....	11
Figure 1.7: Crystal lattice structure of PZT A) Perovskite type lead zirconate titante (PZT) unit cell in the symmetric cubic state in the absence of electric field B) Tetragonally distorted unit cell in the presence of electric field.	21
Figure 1.8: A) Aligned dipoles in single crystal piezoelectric materials, B) Dipoles aligned in different local domains in polycrystalline ceramic piezoelectric materials, C) Strong electric field applied along the desired alignment direction.	22
Figure 2.1: Structure of DGEBA epoxy (Matrix).....	27
Figure 2.2: Steps of purification of CNTs.	30
Figure 2.3: Scheme of preparation of composites.	32
Figure 3.1: Combined XRD pattern of (A) PZT, (B) MWCNTs and (C) epoxy/CNT/PZT composite.....	34
Figure 3.2: DSC thermogram of ODA cured epoxy.	37
Figure 3.3: DSC thermogram of epoxy/CNT composite E-0-0.....	37
Figure 3.4: DSC thermogram of epoxy/CNT/PZT composite E-1-10.....	38
Figure 3.5: DSC thermogram of epoxy/CNT/PZT composite E-1-20.....	38
Figure 3.6: DSC thermogram of epoxy/CNT/PZT composite E-1.5-10.....	39
Figure 3.7: DSC thermogram of epoxy/CNT/PZT composite E-1.5-30.....	39
Figure 3.8: DSC thermogram of epoxy/CNT/PZT composite E-2-20.....	40
Figure 3.9: DSC thermogram of epoxy/CNT/PZT composite E-2-30.....	40
Figure 3.10: TGA thermograms of cured epoxy, epoxy/CNT composite and epoxy/CNT/PZT composite.....	43
Figure 3.11: Combined TGA thermograms of composites by varying CNT loading.....	43
Figure 3.12: Combined TGA thermograms of epoxy/CNT/PZT composites of different PZT loading.	44
Figure 3.13: Typical stress-strain curve for polymers.	45
Figure 3.14: Stress-strain curve of cured epoxy.	46

Figure 3.15: Stress-strain curve of epoxy/CNT composite E-1-0.....	46
Figure 3.16: Stress-strain curve of epoxy/CNT/PZT composite E-1-10.	47
Figure 3.17: Stress-strain curve of epoxy/CNT/PZT composite E-1-20.	47
Figure 3.18: Stress-strain Curve of Epoxy/CNT/PZT composite E-1-30.....	48
Figure 3.19: Stress-strain curve of epoxy/CNT/PZT composite E-1.5-10.....	48
Figure 3.20: Stress-strain Curve of epoxy/CNT/PZT composite E-1.5-20.....	49
Figure 3.21: Stress-strain curve of epoxy/CNT/PZT composite E-1.5-30.....	49
Figure 3.22: Stress-strain curve of epoxy/CNT/PZT composite E-2-10.	50
Figure 3.23: Stress-strain curve of epoxy/CNT/PZT composite E-2-20.	50
Figure 3.24: Stress-strain curve of epoxy/CNT/PZT composite E-2-30.	51
Figure 3.25: Toughness of composites with increasing CNTs loading.	52
Figure 3.26: Toughness of composites with increasing PZT loading.....	53
Figure 3.27: Effect of CNT loading on Young’s modulus of composites.	55
Figure 3.28: Effect of PZT loading on Young’s modulus calculated for different composites.	55
Figure 3.29: Values of stress at break for different composites against CNT loading.	57
Figure 3.30: Calculated values of stress at break for different composites against PZT loading.	57
Figure 3.31: Values of ultimate tensile strength against CNT loading.....	59
Figure 3.32: Values of ultimate tensile strength against PZT loading.	59
Figure 3.33: Values of electrical conductivities as a function of CNT loading.	61

List of tables

Table 1.1: Values of $\tan \delta$ for different materials.	23
Table 2.1: List of Chemicals used.....	27
Table 2.2: Specifications of DGEBA epoxy.	28
Table 2.3: Specifications of MWCNTs (filler).	28
Table 2.4: Specifications of PZT.	28
Table 2.5: Composition of the composites prepared.....	29
Table 3.1: Calculated Glass transition temperature (T_g) of all the composites.	36
Table 3.2: TGA data showing various parameters calculated from thermograms.	42
Table 3.3: Values of toughness calculated for all composites.	52
Table 3.4: Calculated values of Young's modulus for all composites.	54
Table 3.5: Calculated values of stress at break for different composites.	56
Table 3.6: Calculated values of ultimate tensile stress for all composites.	58
Table 3.7: Calculated electrical conductivities for all composites.....	61

1.1 Composite materials

A composite material is made by combining two or more materials often ones that have very different properties. These two materials work together and gives the composite unique properties [1]. In composite materials the constituents maintain their constitutive identities, yet their combination produces properties and characteristics that are different from the constituents. One of these constituents forms a continues phase called matrix and the other one is a reinforcement material, that is in general added to the matrix to improve or alter the matrix properties. The reinforcement forms a discontinuous phase that is dispersed uniformly throughout the matrix. Composites offer several advantages such as,

- They have higher specific strength than nonmetals, alloys and metals.
- They have lower value of specific gravity in general.
- Their stiffness is improved.
- They maintain their weight at high temperatures.
- Their toughness is improved.
- Their fabrication is cheaper.
- Creep and fatigue strength is better.
- Controlled electrical conductivity is possible.
- They are corrosion and oxidation resistant.

1.1.1 Matrix phase

The role of matrix in composite materials is to give shape to the composite part, protect the reinforcements from the environment, transfer loads to reinforcements and toughness of material, together with reinforcements [1]. There are three types of

composites on the basis of matrix used which are metal matrix composites (MMCs), ceramic matrix composites (CMCs) and polymer matrix composites (PMCs). In metal matrix composites (MMCs) the metal is used as matrix, commonly used metals are aluminum, magnesium and titanium. In ceramic matrix composites (CMCs) ceramic matrix is used such as alumina, calcium and aluminosilicate. The advantages of CMCs include high strength, hardness, high service temperature limits for ceramics, chemical inertness and low density. The other class of composites are polymer matrix composites (PMCs) in which polymeric material is used as a matrix. Polymer matrix composites are most widely used class of composites.

1.1.2 Reinforcement phase

The role of reinforcements in composites is to give strength, stiffness, high mechanical properties and to improve other properties such as coefficient of thermal extension, conductivity and thermal transport [2]. On the basis of reinforcements composites can be fibrous, particulates or laminates. Fibrous composites consist of matrices reinforced by short (discontinuous) or long (continuous) fibers. Fibers are generally anisotropic. Examples include carbon, glass, aramid fibers. Particulate composites consist of particles immersed in matrices such as alloys and ceramics. They are usually isotropic because the particles are added randomly. Particulate composites have advantages such as improved strength, increased operating temperature, oxidation resistance, etc. Typical examples include use of aluminum particles in rubber, silicon carbide particles in aluminum, and gravel sand, and cement to make concrete. Laminates consist of flat reinforcements of materials. Typical laminate materials are glass, mica, alumina and silver. Laminate composites provide advantages such as high flexural modulus, higher strength and low cost. However flakes cannot be oriented easily and only a limited number of materials are available for use [3].

Wood is a natural composite of cellulose fibers in a matrix of lignin. Most primitive man made composite materials were straw and mud combined to form bricks for building construction. Reinforced concrete is another example of composite material. The steel and concrete retain their individual identities in the finished structure. However, because they work together the steel carries the tension loads and concrete carries the compression loads most advanced examples perform routinely on spacecraft in demanding environments. Advanced composites have high-performance

fiber reinforcements in a polymer matrix material such as epoxy. Examples are graphite/epoxy, Kevlar/epoxy and boron/epoxy composites. Advanced composites are traditionally used in the aerospace industries, but these materials have now found applications in commercial industries as well.

1.2 Polymer matrix composites

The most common advanced composites are polymer matrix composites. These composites consist of a polymer thermoplastic or thermosetting as matrix material. These materials can be fashioned into a variety of shapes and sizes. They provide great strength and stiffness along with resistance to corrosion. The reason for being most common is their low cost, high strength and simple manufacturing principles [4].

1.2.1 Thermosetting polymers as matrix material

Thermoset is a hard and stiff cross linked material that does not soften and cannot be molded when heated. Due to their stiffness thermosets do not stretch the way that elastomers and thermoplastics do. Several types of polymers have been used as matrices for natural fiber composites. Most commonly used thermoset polymers are epoxy resins [5-9], unsaturated polyester resins [10, 11], Vinyl Ester resins [12-14], Phenolic epoxy resins [15-17], Novolac resin [18] and Polyamides [19-21]. Unsaturated polyesters are extremely versatile in properties and applications and they have been used as the popular polymer matrix in composites. They are widely produced in industries as they have many advantages compared to other thermosetting resins such as room temperature cure capability, good mechanical properties and transparency.

1.2.2 Thermoplastic polymers

Thermoplastics are polymers that require heat to make them process able. Such materials retain their shape when cooled. In addition, these polymers may be melted and transformed into different shapes, often without significant changes in their properties. The thermoplastics which have been used as matrix for composites are as follows [22-24]:

- Chlorinated polyethylene (CPE)
- High density polyethene (HDPE)

- Low density polyethene (LDPE)
- Polypropylene (PP)
- Poly vinyl chloride (PVC)
- Normal polystyrene (PS)
- Mixtures of polymers
- Recycled thermoplastics

1.2.3 Applications of polymer matrix composites (PMCs)

Polymer matrix composites are used for manufacturing:

- **Aerospace structures:** The military aircraft industry has mainly led the use of polymer composites. In commercial airlines, the use of composites is gradually increasing. Space shuttle and satellite systems use graphite/epoxy for many structural parts [25].
- **Marine:** Boat bodies, canoes, kayaks etc.
- **Automotive:** Body panels, leaf springs, driveshaft, bumpers, doors, racing car bodies and so on [26].
- **Sports goods:** Golf clubs, skis, fishing rods, tennis rackets, and so on.
- **War weapons:** Bulletproof vests and other armor parts.
- **Laboratory equipments:** Chemical storage tanks, pressure vessels, piping, pump body, valves, and so on.
- **Biomedical applications:** Medical implants, orthopedic devices, X-ray tables [27].
- **Building Materials:** Bridges made of polymer composite materials are gaining wide acceptance due to their lower weight, corrosion resistance, longer life cycle, and limited earthquake damage.
- **Electrical devices:** Panels, housing, switchgear, insulators, and connectors.

1.3 Epoxy resin as matrix

Epoxy resins are thermosetting polymers that, have one or more oxirane groups or active epoxide at the end(s) of the molecule and a few repeated units in the middle of the molecule [28]. Chemically, they can be any compounds that have one or more 1,2-epoxy groups and can be converted into thermosetting materials. Their molecular weights can vary greatly. They exist either as liquids with lower viscosity or as solids.

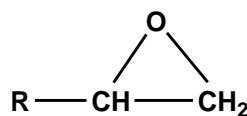


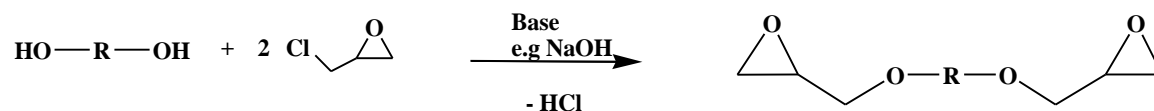
Figure 1.1: Epoxy ring

1.3.1 Types of epoxy resins

On the basis of methods of preparation epoxy resins can be classified into two main classes, glycidyl epoxy resins and non-glycidyl epoxy resins.

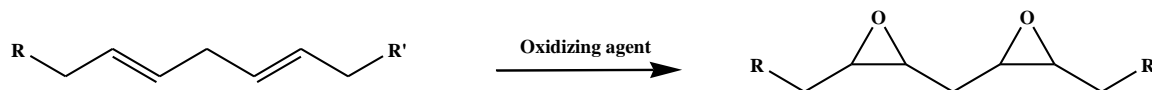
1.3.1.1 Glycidyl epoxy resins

Glycidyl epoxies have epoxide rings at their ends. They are prepared from a reaction between a diol and Epichlorohydrin in the presence of a base. Examples include DGEBA epoxy resin, DGEBF epoxy resin and Novolac epoxy resin.



1.3.1.2 Non-Glycidyl epoxy resins

In Non-Glycidyl epoxies epoxide group is present somewhere inside the chain of a non-glycidyl epoxy molecule. These resins are prepared by the oxidation of alkenes in the presence of suitable oxidizing agent such as per acetic acid.



1.4 Diglycidyl ether of Bisphenol-A (DGEBA)

Diglycidyl ether of bisphenol-A, commonly known as DGEBA epoxy resin is the most commonly used epoxy resin, it is prepared by the reaction of bisphenol-A with epichlorohydrin. Different parameters of the resin like viscosity, physical appearance etc., depend upon the degree of polymerization and the molecular weight of resin.

However, it has relative low viscosity, physical strength after curing and relatively low production cost which makes it important epoxy system. Several varieties of thermally stable rigid rings are present in biphenols which are used to make high performance epoxy resins. Resins which are produced by rigid rings have char formation and improved heat resistance [29].

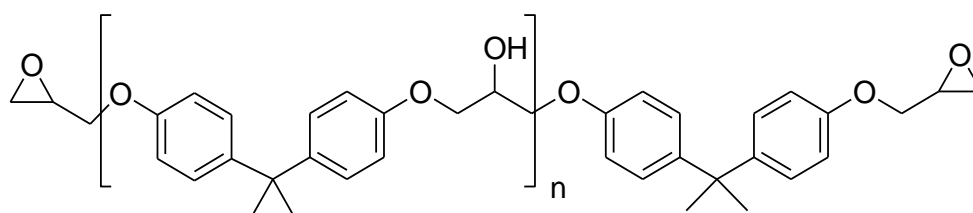


Figure 1.2: Structure of DGEBA epoxy.

1.4.1 Synthesis of DGEBA epoxy

It is prepared by a reacting Bisphenol A with epichlorohydrin in the presence of a base and condensation reaction occurs and, a molecule of HCl is removed. DGEBA undergoes polymerization and forms epoxy resin.

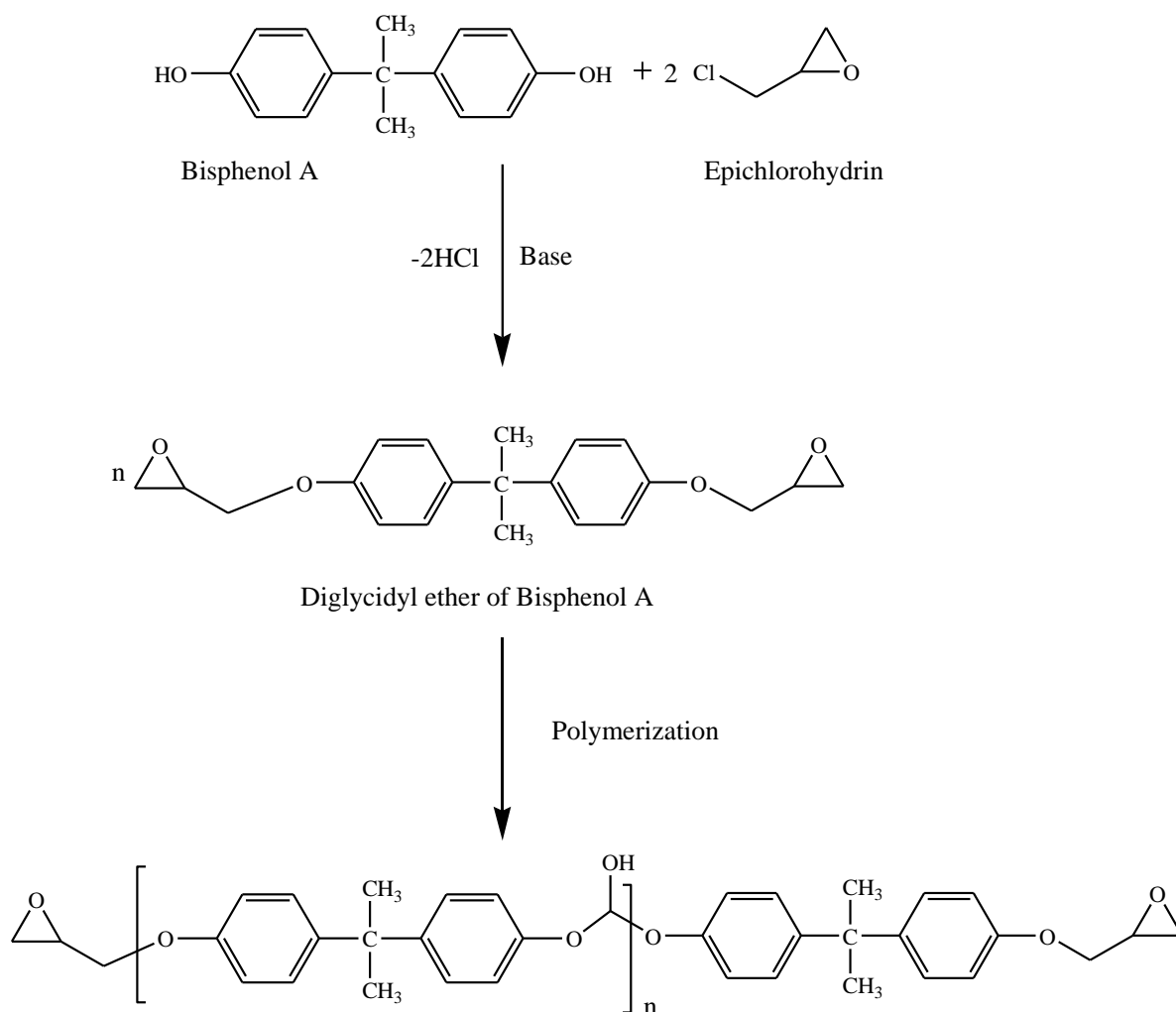


Figure 1.3: Synthesis of DGEBA epoxy.

1.4.2 Curing of epoxy

Curing is a process in which small molecules combine to form a three dimensional network, during the process of curing the mobility of the molecules decreases due to increase in cross linking density that hinders molecular movement, as a result a viscous liquid is converted into a hard solid. Curing of epoxy resin is done by using a curing agent or hardener. During the curing process irreversible changes occurs in the epoxy resin. Glass transition temperature and cure kinetics of epoxy resins depend upon the molecular structure of the curing agent [30]. The degree of cure depends upon the extent of cross-linking. Maximum cross-linking gives the basic important properties. The ultimate cross-linking density is influenced by the curing temperature [31].

1.4.3 Cross linking Density

The number of cross links per volume of the material defines the crosslinking density. Mass of the molecular segments between the cross links and the ratio of curing agent over the epoxy tells about the density of cross link. Cross linking density has some effects on resin system properties which are as under:

- Greater elongation before breakage might be allowed by low crosslinking density through improving toughness (if strength is not significantly lowered) by allowing.
- Low shrinkage during cure can also be the result of a low cross link density.
- Improved resistance to chemical attack can be obtained by high cross linking.

Increase in the heat distortion temperature and glass transition temperature is obtained by higher cross link density, the strain becomes lower to failure by too high cross link density (increase in brittleness) [32].

1.4.4 Curing agents

Curing agents play an important role in the curing process of epoxy resin because they relate to the curing kinetics, reaction rate, gel time, degree of cure, viscosity, curing cycle, and the final properties of the cured products. There are three main types of curing agents. The first type of curing agents includes active hydrogen compounds and their derivatives. Compounds with amine, amides, and hydroxyl, acid or acid anhydride groups belong to this type. They usually react with epoxy resin by poly addition to result in an amine, ether, or ester. Aliphatic and aromatic polyamines [33], polyamides, and their derivatives are the commonly used amine type curing agents. The aliphatic amines are very reactive and have a short lifetime. Their applications are limited because they are usually volatile, toxic or irritating to eyes and skin and thus cause health problems [34]. Compared to aliphatic amine, aromatic amines are less reactive, less harmful to people, and need higher cure temperature and longer cure time. Hydroxyl and anhydride curing agents are usually less reactive than amines and require a higher cure temperature and more cure time. They have longer lifetimes. Polyphenols are the more frequently used hydroxyl type curing agents. Polybasic acids and acid anhydrides are the acid and anhydride type curing agents that are widely used in the coating field.

The second type of curing agents includes the anionic and cationic initiators. They are used to catalyze the homo polymerization of epoxy resins. Molecules, which can provide an anion such as tertiary amine, secondary amines and metal alkoxides are the effective anionic initiators for epoxy resins. Molecules that can provide a cation, such as the halides of tin, zinc, iron and the fluoroborates of these metals are the effective cationic initiators. The most important types of cationic initiators are the complexes of BF_3 .

The third type of curing agents are called reactive cross linkers. They usually have higher equivalent weights and crosslink with the second hydroxyls of the epoxy resins or by self-condensation. Examples of this type of curing agents are melamine, phenol, and urea formaldehyde resins. Among the three types of curing agents, compounds with active hydrogen are the most frequently used curing agents and have gained wide commercial success [35]. Most anionic and cationic initiators have not been used commercially because of their long curing cycles and other poor cured product properties. Cross linkers are mainly used as surface coatings and usually are cured at high temperatures to produce films having good physical and chemical properties.

1.4.5 Curing reactions

The curing reaction of epoxide is the process by which one or more kinds of reactants, i.e., an epoxide and one or more curing agents with or without the catalysts are transformed from low molecular weight to a highly crosslinked structure. As mentioned earlier, the epoxy resin contains one or more 1, 2-epoxide groups. Because an oxygen atom has a high electronegativity, the chemical bonds between oxygen and carbon atoms in the 1, 2-epoxide groups are the polar bonds, in which the oxygen atom becomes partially negative, whereas the carbon atoms become partially positive. Because the epoxide ring is strained unstable, and polar groups nucleophiles can attack on it, the epoxy group is easily broken. It can react with both nucleophilic curing reagents and electrophilic curing agents.

The curing reaction is the repeated process of the ring opening reaction of epoxides, adding molecules and producing a higher molecular weight and finally resulting in a three dimensional structure. The chemical structures of the epoxides have an important effect on the curing reactions [36]. It was concluded that the electron-

withdrawing groups in the epoxides would increase the rate of reaction when cured with nucleophilic reagents, but would decrease the rate of reaction of epoxides when cured with electrophilic curing agents [37]. A general reaction for curing of epoxy is given below

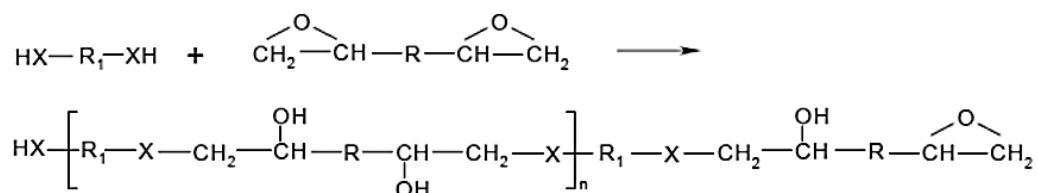


Figure 1.4: General reaction of epoxy curing.

where X represents NR_2 , O or S nucleophilic group or element and n is the degree of polymerization, having a value of 0, 1, 2 ...

Reaction of epoxy and amine

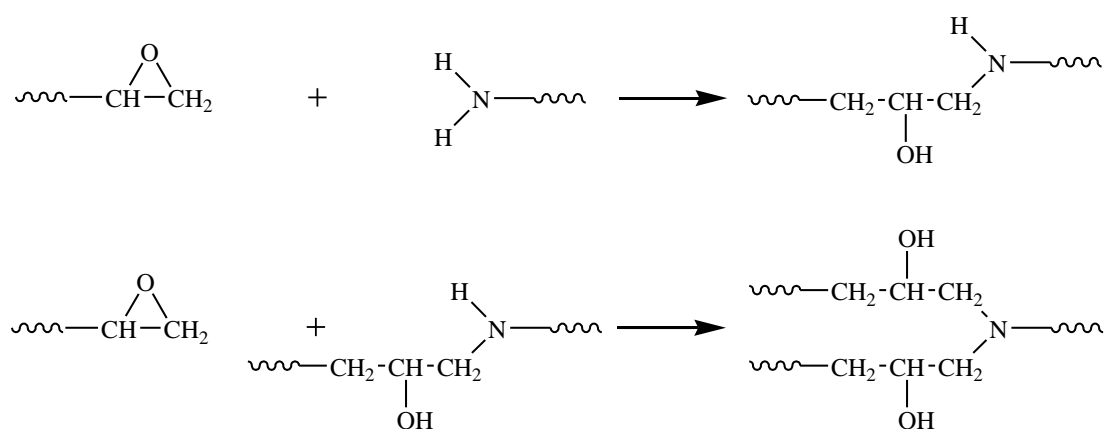


Figure 1.5: General reaction of epoxy and amine.

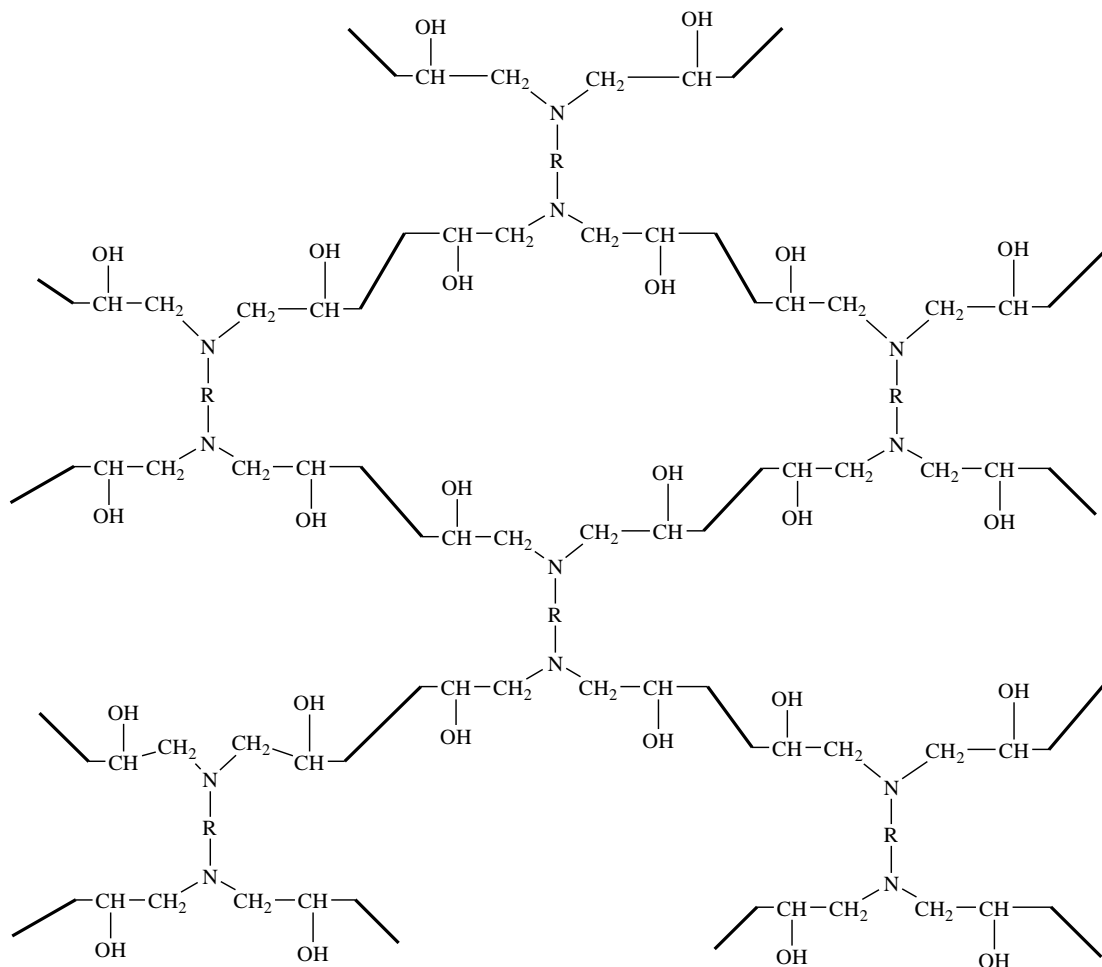


Figure 1.6: Three dimensional network of epoxy.

1.4.6 Selection of curing agents

The selection of curing agents is a critical parameter. There are numerous types of curing agents that can react with epoxy resins. Selection of curing agents affects mechanical properties, glass transition temperature of the epoxy resin for example aromatic amines react slowly with epoxy resins at room temperature and require high temperature for cure. They give better thermal and chemical resistive properties Thermal stability is affected by the structure of the hardener[38]. Selection of curing agent depends upon the conditions and applications of the epoxy, different curing agents give different properties to epoxy.

1.4.7 The stoichiometry

The stoichiometric relationship between curing agents and resins has a great effect on the physical and the mechanical properties of the epoxy resin [39]. The

different types of curing agents requires addressing stoichiometric balance between the reacting species. To evaluate the properties of the epoxy resin the proportions of curing agents and resins must be calculated and optimized. Theoretically, a crosslinked thermoset polymer structure is obtained when equimolar quantities of resin and hardener are combined.

However, in practical applications, epoxy formulations are optimized for performance rather than to complete stoichiometric cures. This is especially true when curing high molecular weight epoxy resins through the hydroxyl groups. In primary and secondary amines cured systems, normally the hardener is used in near stoichiometric ratio, because the tertiary amine formed in the reaction has a catalytic effect on reactions of epoxy with co-produced secondary alcohols. Slightly less amount than the theoretical amounts should be used, often a commercial curing agent's chemical structure is kept proprietary or the amount of reactive functional group is ambiguous. In such cases, the vendor provides an amine or active hydrogen equivalent from which an appropriate mix ratio can be calculated.

While performing stoichiometric balances, it is important to be aware of reactive groups that may be bifunctional (e.g., anhydride, olefin). The stoichiometric ratio of hardener/resin doesn't always produce a cured resin system having optimized properties, where a specific application required properties have been developed through the use of a defined hardener/resin ratio, is different from other application which required different properties i.e. different hardener/resin ratio.

1.4.8 General properties of epoxy resin

1.4.8.1 Chemical resistance

Epoxy thermosets are versatile from the point of view of chemical resistance. Three dimensional cross-link networks are stable in front of the attack of corrosive chemicals, including alkalis, acids, and organic solvents. They are attacked by some strong acids, but they are very resistant to strong alkalis [40]. The chemical resistance of a completely cured resin depends upon its structure and chemical composition, the degree of cross linking and molecular weight.

1.4.8.2 Thermal resistance

Heat resistance is related to resin composition. Molecular weight between crosslinks, degree of crosslinking and chemical structure of the network have direct effects on strength and rigidity at elevated temperatures [41]. The crosslinked nature improves the resistance to deformation and softening at high temperature. The structural transitions of these cross linked networks are characterized with DSC, DMTA or by measuring heat distortion temperature (HDT) [42, 43], these studies give the transition temperature at which amorphous margins transform to a rubbery state. The HDT is a measure of the thermal resistivity of the resin.

1.4.8.3 Mechanical properties

Unmodified epoxy resins shows brittleness and less elongation after curing. These polymers usually fail on their free surface and the failed areas are converted into cracks, which spread with brittle energy absorption which results in fracture. The high T_g (glass transition temperature) of epoxy thermosets are the result of highly cross linked structures and this is achieved at the expense of lowering in toughness and damage tolerance [5].

1.5 Carbon nanotubes (CNTs) as reinforcement

Carbon nanotubes, first time discovered in 1991 [44], are considered to have long, cylindrical sheets of graphite in which the layer of carbon atoms joined together in a hexagonal-honeycomb like structure, this one atom thick layer is termed as graphene layer. CNTs are large molecules having distinguishable size, shape and physical properties. The discovery of these exciting structures led too much advancement in the recent years and extensive studies have been done to explore their properties for the desired applications however, the physical properties are still being discovered. Nanotubes are broadly being used in a wide range of applications i.e. electronic, thermal, structural and mechanical properties depending upon different parameters of CNTS e.g. diameter, length and chirality.

1.5.1 Properties of CNTs

CNTs are the highly promising candidates in the field of nanotechnology having diameter less than 100 nanometers and a thickness of 1-2 nm carbon nanotubes (CNTs)

are the example of real nanotechnology. Their diameter is less than 100 nanometer and thickness up to 1 or 2 cm. CNTs can be used both in physical and chemical aspects thus opening an incredible range of applications in material science, electronics, chemical processing and other fields. Some of the properties are

- Extraordinary electrical conductivity
- Mechanical properties
- Electron field emission (High aspect ratio)
- Very High Tensile Strength
- Highly Flexible- can be bent considerably without damage
- Very Elastic $\approx 18\%$ elongation to failure
- High Thermal Conductivity
- Low Thermal Expansion Coefficient
- Highly modified structure and optimized solubility due to the chemistry of Carbon present in their structure

1.5.2 Applications of CNTS

- Conductive and high-strength composites
- Energy storage and energy conversion devices
- Sensors
- Field emission displays and radiation sources
- Hydrogen storage media
- Nanometer sized semiconductor devices, probes, and interconnects
- Field emitters
- Conductive or reinforced plastics
- Biomedical applications

1.5.3 Single walled carbon nanotubes (SWCNTs)

Single walled carbon nanotubes can be formed in three different designs armchair, chiral and zig zag depending upon the wrapping of graphene layers into a cylinder. Bulk synthesis is difficult as it requires proper control over growth and atmospheric condition and a catalyst is required for their bulk synthesis. Purity is poor

and a chance of defect is more during functionalization. Characterization and evaluation is easy and they can be easily twisted being more pliable.

1.5.4 Multiwalled carbon nanotubes (MWCNTs)

Two models were proposed to define the structure of multiwalled carbon nanotubes. Russian Doll model says that carbon nanotube contains another carbon nanotube inside it having a smaller diameter. Parchment model says that every graphene layer is rolled itself number of times. The properties of MWCNTs resemble to those of SWCNTs, the only significant difference is that the outer layers of graphene in MWCNTs are protecting the inner ones. Other properties which differentiate them from SWCNTs are that they can be produced without catalyst, their bulk synthesis is easy having high purity. A chance of defect is less but once occurred, it is difficult to improve. Their structure is very complex and cannot be easily twisted.

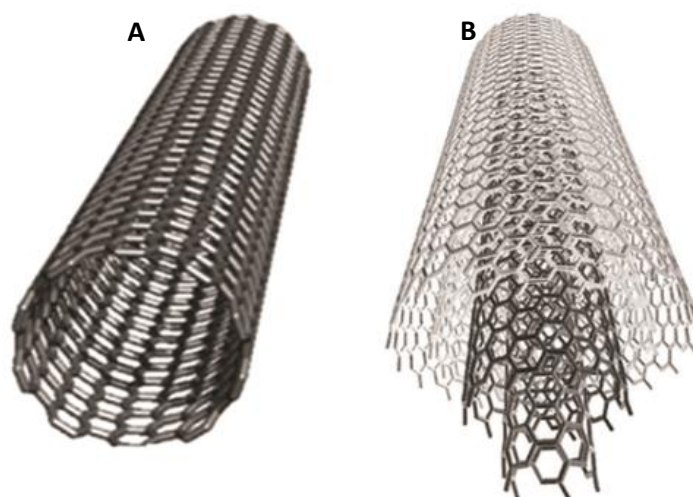


Figure: Schematic diagrams of single-wall carbon nanotube (SWCNT) (A) and multi-wall carbon nanotube (MWCNT) (B) [45].

In recent years, different types of polymer composites have been synthesized by incorporating CNTs into various polymer matrices such as polyamides [46]polyimides [47], epoxy [48-50]polyurethane [51, 52] polypropylene [53, 54], polyethylene [55], polyethylene oxide [56, 57], polyvinyl alcohol [58], polymethyl methacrylate (PMMA) [59], polycarbonate [60], polybutylene succinate [61], polylactide [62], polyaniline [63], polypyrrole [64-66], and others [67]. The problem associated with the use of

CNTs as matrix involves poor dispersion of the CNTs and formation of agglomerations in the composites.

Due to tiny size of the nanostructured nanotubes, their tendency to form agglomerates, and their large surface area per unit volume yields an improved influence of the interfacial bonding on the effective properties of the composite. Due to the intrinsic Van der Waals attraction of the CNTs to each other and high aspect ratio, carbon nanotubes are held together as bundles and ropes having very low solubility in most solvents. When they are blended with the polymer, they remain entangled agglomerates which prevent uniform dispersion of the filler into the polymer matrix. Again, the smooth non-reactive CNT surface limits the load transfer from the matrix to nanotubes. Additional fabrication problems arises due to the increase in viscosity when the CNTs are added directly to the polymer [68]. For CNT composites, the problem is intensified by the influence of tube morphology and content of amorphous carbon and metal impurities normally contained in the CNTs.

These impurities are synthesized along with CNTs, they are frequently removed or reduced by oxidation or addition of groups on CNT surfaces, which causes structural and morphological changes in the tubes [69, 70]. By looking at the potential advantages of using CNTs as reinforcement, several researchers have violently monitored their use in polymer nanocomposites, either thermoplastics or thermosetting [71-73]. CNT based epoxy composites are materials have gained high technological interest due to their interesting features such as their mechanical strength, thermal stability and electrical properties. A large number of recent works have been done with CNT reinforced epoxy.

1.5.5 Epoxy containing MWCNTs

The excellent property of mechanical strength allows MWCNTs to be used as possible reinforcing materials, MWCNTs reinforcement would produce electrically conductive, very strong and light materials. These properties of MWCNTs attracted the attention of scientists in all over the world to incorporate MWCNTs in epoxy matrix for the construction of advanced engineering materials. Following the first report on the fabrication of aligned MWCNTs by cutting epoxy CNTs composites by Ajayan et al. [74] there have been continuous efforts to incorporate CNTs into various types of epoxy resins to fabricate functional composite materials with desirable electrical and mechanical properties. Sandler and co-workers [75] dispersed untreated MWCNTs in

an epoxy matrix by using the process developed for carbon black [76, 77]. The matrix used in this study was an epoxy polymer based on bisphenol-A resin (Araldite LY 556) and an aromatic hardener (Araldite HY 932).

Gong et al.[78] used a non-ionic surfactant for dispersing CNTs in epoxy polymer matrix. The bisphenol-A epoxy resin with hydroxylated polyamine hardener H-91 and the surfactant polyoxyethylene 8-lauryl ($C_{12}EO_8$) were used for the composite preparation. Other researchers used ultrasonication for the dispersion of CNTs in the epoxy matrix. For example, Lau and co-workers [50] used different weight fractions of MWCNTs, into the epoxy resin (Araldite GY 251) by using ultrasonication of resin with ethanol solution containing CNTs for 2 hours. The composites were heated to dry in vacuum oven for two days to remove air bubbles and the solvent. Like previous authors, Park et al. [79] also employed the sonication method to disperse CNTs in the epoxy matrix. In their experimental procedure, the MWCNTs (0.1, 0.5 and 2 vol.%) were first sonicated with methanol based epoxy solution for 2 h, and then sonication was done for 6 h at 35 °C to remove the solvent. The samples were then dried in a vacuum oven at 50 °C for 7 days.

In another report, Wong et al. [80] fabricated CNT/epoxy thin film by using spin coating technique. Their major objective was to study the interfacial morphology of CNT epoxy composite. A standard 4 inch silicon cracker was used to spin coat the mixture of MWCNTs and epoxy resin (Epon SU-8). After curing the composite film system, the substrate was etched from the backside by deep reactive ion etching (DRIE).

Park et al. [81] used oxyfluorinated-MWCNTs (synthesized using the CVD process) to reinforce epoxy matrix. The objective was to study the effect of oxyfluorinated MWCNTs surfaces on the-mechanical and interfacial properties of resulting composites. In a typical experimental procedure, MWCNTs outer surfaces were functionalized with F_2 , O_2 and N_2 gases in a batch reactor made of nickel at a pressure of 0.2 MPa with reaction time of 15 min. Surface analysis results with Fourier transform infrared spectroscopy (FT-IR) and X-ray diffraction (XRD) showed fluorine oxygen contents and –OH groups on MWCNT surfaces were maximized at 100°C. For the preparation of composite, the epoxy resin (diglycidyl ether of bisphenol-A DGEBA, YD-128) was mixed with 0.5 wt% of treated MWCNTs and sonicated for 3 h at 60°C. After adding the hardener diaminodiphenylmethane (DDM), the mixture was stirred

thoroughly, degassed to remove bubbles and molded. The samples were cured for 2 h at 120 °C, 2 h at 150 °C and finally, 1 h at 200°C. Results show that the mechanical and mechanical interfacial properties of the resulting composites were improved with increasing F-O content. This indicates that polar groups such as fluorine and oxygen increases the wet ability of CNTs surface with the epoxy matrix.

To study the effect of MWCNTs aspect ratio on the properties of final composites, Pumera et al. [82] fabricated MWCNTs/epoxy composites with two different types of MWCNTs. Both types of MWCNTs (CNT-200: length, 0.5–200 µm; diameter, 30–50 nm; wall thickness, 12–18 nm and CNT-2: length 0.5–2 µm, diameter 20–30 nm, wall thickness 1–2 nm) were produced by the CVD technique. The purification was accomplished by stirring the CNTs in 2 M HNO₃ at 25°C for 24 h. Epoxy resin Epotek H77A and hardener Epotek H77B were mixed manually in the ratio 20:3 (w/w) using a spatula. CNT electrodes have been produced by loading the epoxy resin, before curing, with different amounts [i.e., 10, 12.5, 15, 17.5 and 20% (w/w)] of CNTs and mixed for 30 min. The composite was cured at 40°C for 1 week, results showed good dispersion of CNTs in the polymer matrix in general when compared to the conventional graphite epoxy composite.

Over the last few years, the potential use of MWCNTs as conducting fillers to improve the electrical conductivity of epoxy matrix has been established. Several authors have reported significant enhancement in electrical conductivity with a very small loading of MWCNTs in the epoxy matrix, while maintaining the mechanical performance of composites. Sandler et al. [75] reported the electrical conductivity of an epoxy matrix containing untreated CNTs around 10⁻² Sm⁻¹ at a filler content of 0.1 vol% which is much higher compared to the composite containing conventional carbon black filler. The conductivity showed gradual increase with CNT content. The percolation threshold was found to be in between 0.0225 and 0.04 vol% of CNTs.

Park et al. [79] also found that the resistivity of composite decreased with CNT content, and the threshold concentration reached 0.5 vol.% of CNTs. However, Cui et al. [83] reported a relatively high percolation threshold around 8 wt% of CNTs for two series of epoxy composites prepared with and without surfactant from D.C. resistivity measurements. The wrapping of the CNT surface by the surfactant prevents particle-particle interaction and contributes to the high critical wt% of the filler to attain

percolation network. On the other hand, Sandler and co-workers [76] suggested the use of aligned MWCNTs to get a uniquely low percolation threshold. CNT concentration of about 0.0025 wt% was found to be enough to produce the conducting network within the epoxy matrix in this case.

Martin et al. [84] reported similar results in another work. The bulk conductivity values varied from dielectric nature to 10^{-3} Sm^{-1} depending on the nanotube aggregation and dispersion levels obtained under various processing conditions. According to them, the processing parameters should be carefully adjusted to achieve very low percolation threshold. Moisala et al. [85] also prepared conductive epoxy composite with MWCNTs with a percolation threshold of 0.0025 wt% using high shear mixing procedure proposed by Sandler et al. [76].

1.6 Piezoelectric materials

Piezoelectric materials are nonconductive materials that have ability to generate electric charges when they are subjected to mechanical stress, such as those caused by sound vibration and pressure [86-88], the amount of electric charges are proportional to the amount of mechanical stress applied, these materials can also generate mechanical vibrations when they are subjected to an electric field. These materials have no crystalline inversion symmetry and there exists a linear interaction between the mechanical energy and electrical energy [89]. The piezoelectric effect is a reversible process it has two types one is called direct effect in which electrical potential field is generated in response to applied mechanical stress, on the basis of this effect sensors are developed, the other one is called inverse effect in which mechanical vibrations are produced when they are subjected to electric field, this effect is used in actuators where sound is produced in response of electric field.

Piezoelectric materials are used in many devices such as sensors [90-92], actuators [93-97], resonators [98] and transducers [99-101] which convert electrical energy into mechanical energy or vice versa, in capacitors [102, 103] and health monitoring applications [104]. In addition of this piezoelectric materials are also employed in electronic frequency generation, sound detection and sound generation, microbalances, optical instruments, ultrafine focusing, atomic resolution instruments and other devices which require voltage generation and amplification. Piezoelectric materials have also gained interest because of their use as energy harvesting materials

and sound damping devices. They are also used in hybrid energy systems energy harvesting is the process in which energy is derived from ambient waste energy sources, such as vibration, solar energy waste heat etc., they are used for capturing and storing energy for using in electronic systems [87, 105-110].

Piezoelectric ceramics have certain limitations in energy harvesting and acoustic dampening devices [111]. They exhibit poor mechanical properties and they are prone to failure, which limits their applications in acoustic dampening. The brittle nature of these materials make them susceptible to premature failure when they are subjected to frequency dependent mechanical loading and working range of these materials is restricted to a limited band width [112, 113]. These issues can be resolved by introducing piezoelectric composites that is the composites which contains piezoelectric materials as filler or reinforcement. Polymer based piezoelectric composites are best for these applications in which mechanical vibration energy is transmitted to a piezoelectric material and in turn mechanical energy is converted into electrical energy by piezoelectric effect, the electric potential is then converted into joule heat by network of conductive particles in the polymer matrix this process is known as piezoelectric damping effect, it depends upon the electrochemical properties of composites [114].

1.6.1 Piezoelectric materials and electromechanical properties

Piezoelectric material produce an effective electric field on applying mechanical strain. When an electric field is applied across piezoelectric material it results in a mechanical strain or deformation [95, 114, 115]. Many materials in nature exists as piezoelectric materials such as quartz, topaz etc. and manmade such as Barium Titanate(BaTiO_3) [116-119], Lead Zirconate Titanate (PbZrTiO_3) exhibit excellent piezoelectric properties [92, 120, 121]. Piezoelectric effect is due to the formation of crystal lattice structures that have no center of symmetry.

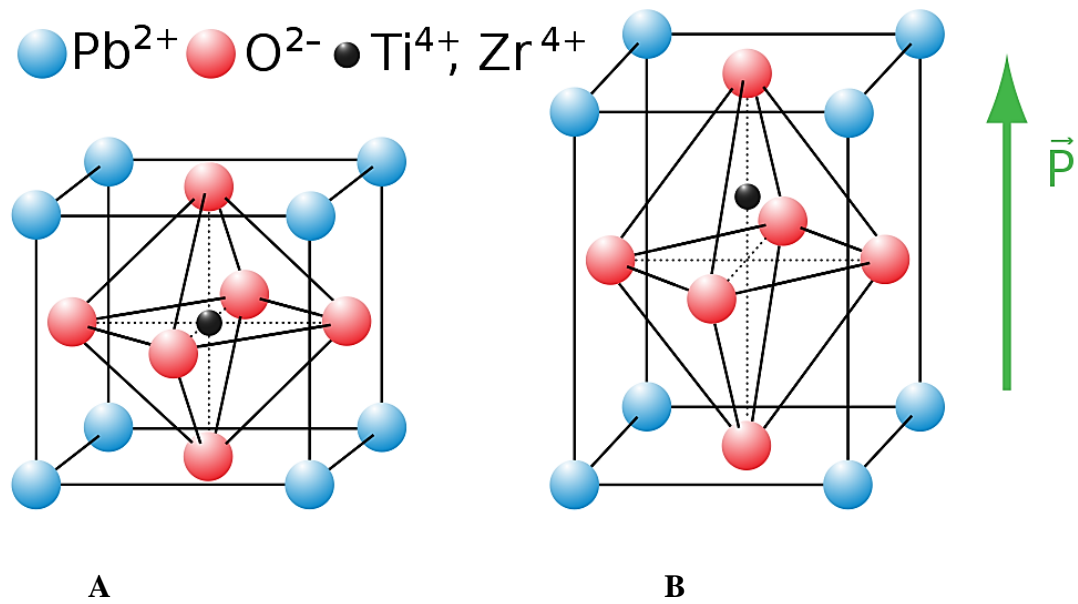


Figure 1.7: Crystal lattice structure of PZT A) Perovskite type lead zirconate titanate (PZT) unit cell in the symmetric cubic state in the absence of electric field B) Tetragonally distorted unit cell in the presence of electric field.

In unit cell of Piezoelectric crystal the dipoles are formed due to which asymmetry is created, the unit cell has perovskite structure. In perovskite structure there are two crystallographic forms. It is in asymmetric distorted tetragonal unit cell below Curie temperature and the temperature is above Curie temperature they converted into a cubic structure. In the tetragonal state each unit cell has an electric dipole, there is a charge differential between each end of unit cell, this arises due to the displacement of the central atom in case of PZT the central atom is Ti or Zr. For single crystal piezoelectric materials the dipoles are aligned in same direction for polycrystalline ceramics, such as PZT the dipoles are aligned along certain local domains, when an electric field is applied across the material, these dipoles are aligned along a certain direction, this process is called poling.

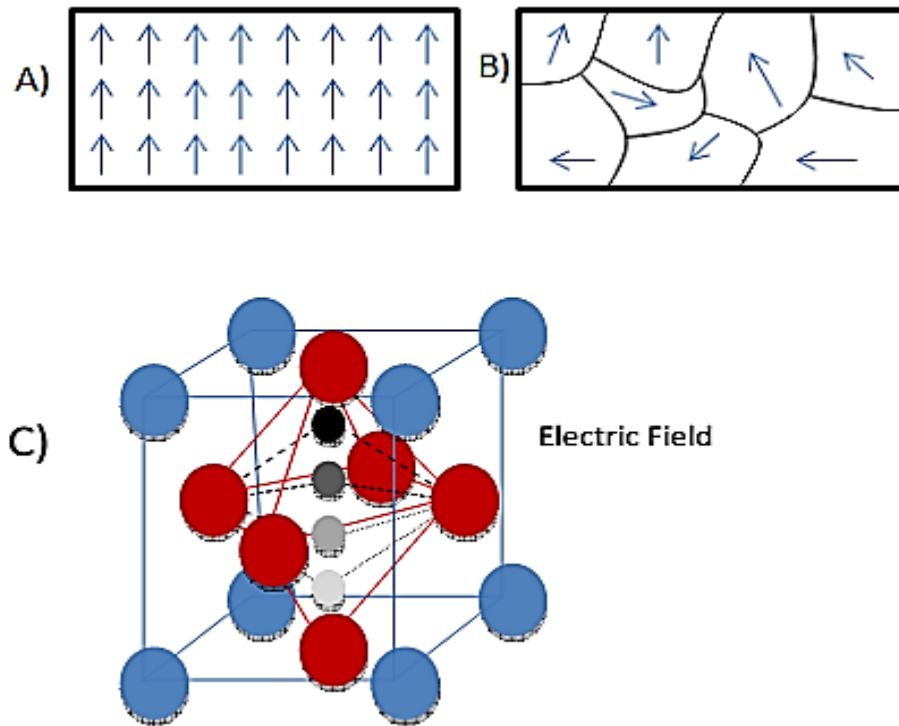


Figure 1.8: A) Aligned dipoles in single crystal piezoelectric materials, B) Dipoles aligned in different local domains in polycrystalline ceramic piezoelectric materials, C) Strong electric field applied along the desired alignment direction.

The relationships between applied forces and the amount of electric current depends upon the piezoelectric properties of the ceramic, the size and shape of the material and direction of the electrical and mechanical excitation. This relationship is quantified by using electromechanical coefficients. The equation for piezoelectric material can be expressed as

$$D = \epsilon^T E + dT \quad (i)$$

$$S = S^E T + dE \quad (ii)$$

Where S is the-strain, T is the stress, S^E is the elastic compliance at constant electric field, E is the electric field, D is the electric charge displacement, ϵ^T is dielectric constant at a constant stress, and d is piezoelectric strain constant. Electromechanical coefficients such as s, d, ϵ relate both to the direction of the applied mechanical or electrical excitation and direction of response. Each coefficient has two subscripts that relate to the directions of the two related quantities. To express polarization generated

per unit mechanical stress piezoelectric strain coefficient is used which is shown as d_{ij} (where $i, j = 1, 2, 3, \dots$) it also shows mechanical strain induced per unit electric field applied.

The performance of piezoelectric materials can be examined by several properties such as relative permittivity or dielectric constant, it is the amount of charge that the material can store. The other factor known as Electromechanical coupling factor k_{ij} indicates effectiveness with which a piezoelectric material converts electrical energy into mechanical or mechanical into electrical, the subscript k denotes the direction along which the electrodes are applied and ij represents the direction along which the mechanical energy is applied or developed. The $\tan \delta$ is the tangent of the dielectric loss angle δ , and it is determined by the ratio of effective conductance to effective susceptance in a circuit which is measured by using an impedance bridge. It is an important parameter for the characterization of the viscoelasticity of the material. It represents damping capacity of material which is the ability of a piezoelectric material to convert mechanical energy into electrical energy or heat energy when they are subjected to any external load, basically δ is the phase angle between stress:

$$\tan \delta = \frac{|E| \sin(\delta)}{|E| \cos(\delta)} = \frac{E''}{E'} \quad (\text{iii})$$

Where E' shows elastic storage modulus and E'' shows elastic loss modulus. The storage modulus is the amount of mechanical energy stored during deformation and the loss modulus is the energy lost in the form of heat during the deformation cycle. Damping capacity for a piezoelectric material is very important for their performance it represents the amount of energy dissipated as heat and electricity during one cycle of mechanical vibration following table shows the values ranges of $\tan \delta$ for different materials.

Table 1.1: Values of $\tan \delta$ for different materials.

Material	$\tan \delta$
Structural Ceramics	10^{-4} to 10^{-5}
Structural metal	0.001 to 0.01
Melamine foams	0.01 to 0.11
Piezoelectric materials	0.01 to 0.9
Natural rubber an viscoelastic polymers	>2

1.6.2 Piezoelectric composites:

Piezoelectric composites comprised of piezoelectric material embedded in a polymer matrix, they are widely used in passive devices such as capacitors [122]. Piezoelectric polymer composites are gaining much attention due to their flexibility and ease of processing these composites can be used in acoustics and transducers. Transducers are the devices which convert one form of energy into other i.e. electrical into mechanical or vice versa. Performances of piezoelectric composites depends upon the piezoelectric coefficient of the material and electrical conductivity of the composites, electrical conductivity of the composites can be enhanced by inclusion of conductive fillers [123]. Inclusions of electrically conductive fillers within polymer matrices have been demonstrated by several researchers [124]. All researchers have reported that the polymer matrix conductivity was enhanced by the electrically conductive fillers [73, 74]. Recently Carbon Nanotubes (CNTs) has emerged as an attractive filler material due to its electrically conductive nature and high aspect ratio [125].

Composites with carbon nanotubes embedded in a polymer matrix have been studied by researchers [49, 126, 127]. The dielectric properties of these composites are enhanced due to the increase in charge carriers from the carbon nanotubes. However beyond a certain volume fraction of the CNTs, the composite reaches percolation threshold due to the formation of electrically conductive pathways in the composite, and there is a sharp rise in the conductivity. Ma and Wang [128] compared the microstructure and dielectric properties of epoxy based damping composites that contained carbon nanotubes (CNTs) and PMN-PZT piezo ceramics. They concluded that the composites exhibited a percolation threshold in the range of 1.0–1.5 g CNTs per 100 g epoxy. They also concluded that in the region of the percolation threshold, a continuous electro conductive network was formed, and that beyond the percolation threshold, these materials demonstrated dynamic mechanical loss factors that were superior to those below the percolation threshold, and those without semiconductive inclusions.

Tian and Wang [129] also examined the performance of epoxy multiwalled carbon nanotube piezoelectric ceramic composites as rigid damping materials. Their results were similar to Ma and Wang [55], where the percolation threshold was found to be in the range of 1.0–1.5 g CNTs per 100 g epoxy. They too concluded that loss

factors were improved with the incorporation of CNT and PZT, where the amount of CNT was above the critical electrical percolation loading. Researchers have predicted that the increase in the volume fraction of the electrically conductive inclusion phase in composite can also lead to an increase in conductivity [124, 130].

1.7 Present work

To prepare the Epoxy based composites containing Multiwalled carbon-nanotubes (MWCNTs) and Lead Zirconate Titanate (PZT). Carbon nanotubes act as a conducting medium and disperse the electric current produced by PZT in response to any mechanical stress hence these composites behave as piezoelectric composites and can be used as energy harvesting materials in various aspects of life.

Piezoelectric materials are used to convert electrical energy into mechanical and vice versa these materials are used as sensors and actuators where a little amount of energy is produced these materials are not used as energy producing devices the reason behind that fact is they do not produce sufficient amount of electric current to derive any instrument and due to their brittle nature they decompose or fracture when they are subjected to any load or they have poor fracture resistance. The other reason is their insulating nature, due to which the electric current produced is not dispersed throughout the crystal so they cannot be made into sheets or they cannot be used for what they are supposed to be.

1.7.1 Strategies developed

To overcome the above mentioned problems and to utilize piezoelectric materials for the production of electrical energy these materials were drawn into composites. To prepare piezoelectric composites a conductive filler having good electrical conductivities and high aspect ratio is needed and a matrix having good mechanical properties. The polymer matrix used was epoxy resin with 4'4 Oxidianiline as hardener or curing agent, Multiwalled carbon nanotubes were used as a conductive medium for the conduction and dispersion of electric current produced by piezoelectric material, Carbon nanotubes have excellent electrical properties and high aspect ratio also they have good mechanical properties. Lead Zirconate Titanate (PZT) was used as piezoelectric material for the conversion of mechanical energy into electrical energy, PZT have excellent piezoelectric properties among all manmade piezoelectric

materials. To obtain piezoelectric composites having improved conductivity the carbon nanotubes used were non-functionalized because the electrical conductivity of carbon nanotubes reduces by functionalization. Non-functionalized carbon nanotubes were dispersed by ultra-sonication for 2-3 hours, improved electrical conductivity was obtained.

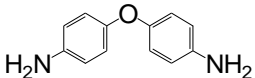
To study the effect of addition of fillers on the matrix and to study the effect of both fillers on the performance of piezoelectric composites, different formulations were developed by varying the weight percent of Carbon nanotubes and PZT.

Addition of carbon nanotubes into epoxy matrix changes the insulating nature of epoxy matrix and act as a conducting medium, Lead Zirconate Titanate (PZT) incorporated into epoxy matrix gives piezoelectric properties to composites. Carbon nanotubes were expected to increase the electrical conductivity of the composites and also improves the mechanical properties and thermal stability of the epoxy matrix. PZT were expected to improve dampening of the epoxy matrix.

2.1 Chemicals

The names, formulas and structures of the chemicals used is given below:

Table 2.1: List of Chemicals used.

Name	Formula	Purity (%)	Source
4-4' Oxydianiline (ODA)		98	Alfa Aesar
N,N' Dimethylacetamide (DMAc)	CH ₃ CON(CH ₃) ₂	99.8	Aldrich
Sulphuric Acid	H ₂ SO ₄	95-97	Fluka

2.2 Specifications of matrix and reinforcement used in the study

Diglycidyl ether of bisphenol-A epoxy resin was used as matrix in this study. The structure of the epoxy is given below:

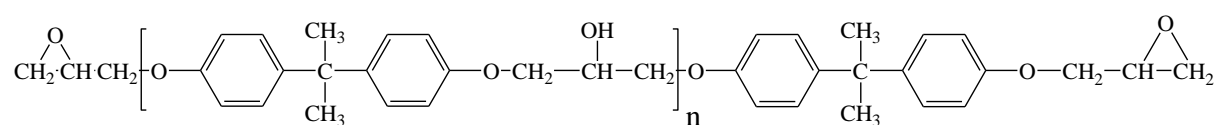


Figure 2.1: Structure of DGEBA epoxy (Matrix).

The specifications of Diglycidyl ether of Bisphenol-A (DGEBA) are given below:

Table 2.2: Specifications of DGEBA epoxy.

Name	Degree of polymerization	Physical Appearance	Number Average Molecular Weight	Epoxide Equivalent Weight
Epoxy resin	1.09	Viscous Liquid	442	221

2.3 Specifications of Multiwalled Carbon nanotubes

Carbon nanotubes used as filler in this study had following specifications:

Table 2.3: Specifications of MWCNTs (filler).

Type	Purity	Diameter	Electrical Conductivity	SKU #
Multiwalled Carbon Nanotubes	95wt%	20-30nm	1000 Sm ⁻¹	sku-030104

2.4 Specifications of PZT

Table 2.4: Specifications of PZT.

Physical property	Metric
Density	7.0-8.0 g/cc
Young's Modulus	50.5 GPa
Piezoelectric Coefficient	425-500 pC/N
Particle size	1.0 µm

Different formulations were developed by varying the weight ratios of the fillers i.e. CNTs and PZT, composition and sample codes are given below in table 2.5.

Table 2.5: Composition of the composites prepared.

S:no.	Sample Code	Epoxy	CNT (weight ratios)	PZT (weight ratios)
1	E-0-0	1	0.000	0.0
2	E-1-0	1	0.010	0.0
3	E-0-10	1	0.000	0.1
4	E-1-10	1	0.010	0.1
5	E-1-20	1	0.010	0.2
6	E-1-30	1	0.010	0.3
7	E-1.5-10	1	0.015	0.1
8	E-1.5-20	1	0.015	0.2
9	E-1.5-30	1	0.015	0.3
10	E-2-10	1	0.020	0.1
11	E-2-20	1	0.020	0.2
12	E-2-30	1	0.020	0.3

The Experimental work is divided into two steps each step is discussed in detail below:

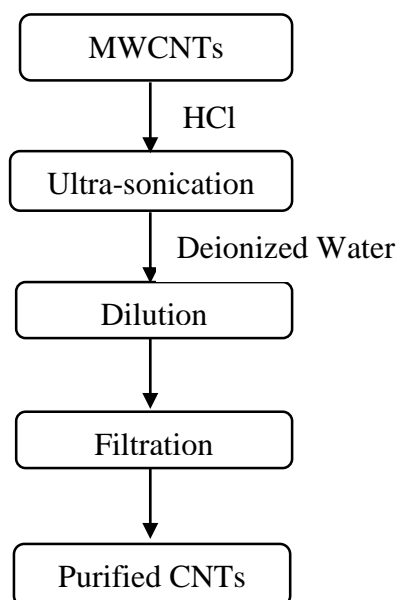
2.5 STEP-1

2.5.1 Purification of carbon nanotubes

Carbon nanotubes used were 95% pure. They contain graphene, fullerenes, amorphous carbon and metal particles as impurities [131] so it was necessary to purify carbon nanotubes, purification was done by using a physical method of purification [132].

Multiwalled carbon nanotubes were soaked into HCl, for 3 gram CNT's 30 mL HCl was used and subjected to ultra-sonication for 3 hours, the acid dissolves metal particles present in the CNT's, after sonication they were diluted with deionized water followed by vacuum filtration, fullerenes and amorphous carbon particles get separated here and purified carbon nanotubes were obtained. The scheme of CNTs purification is given below:

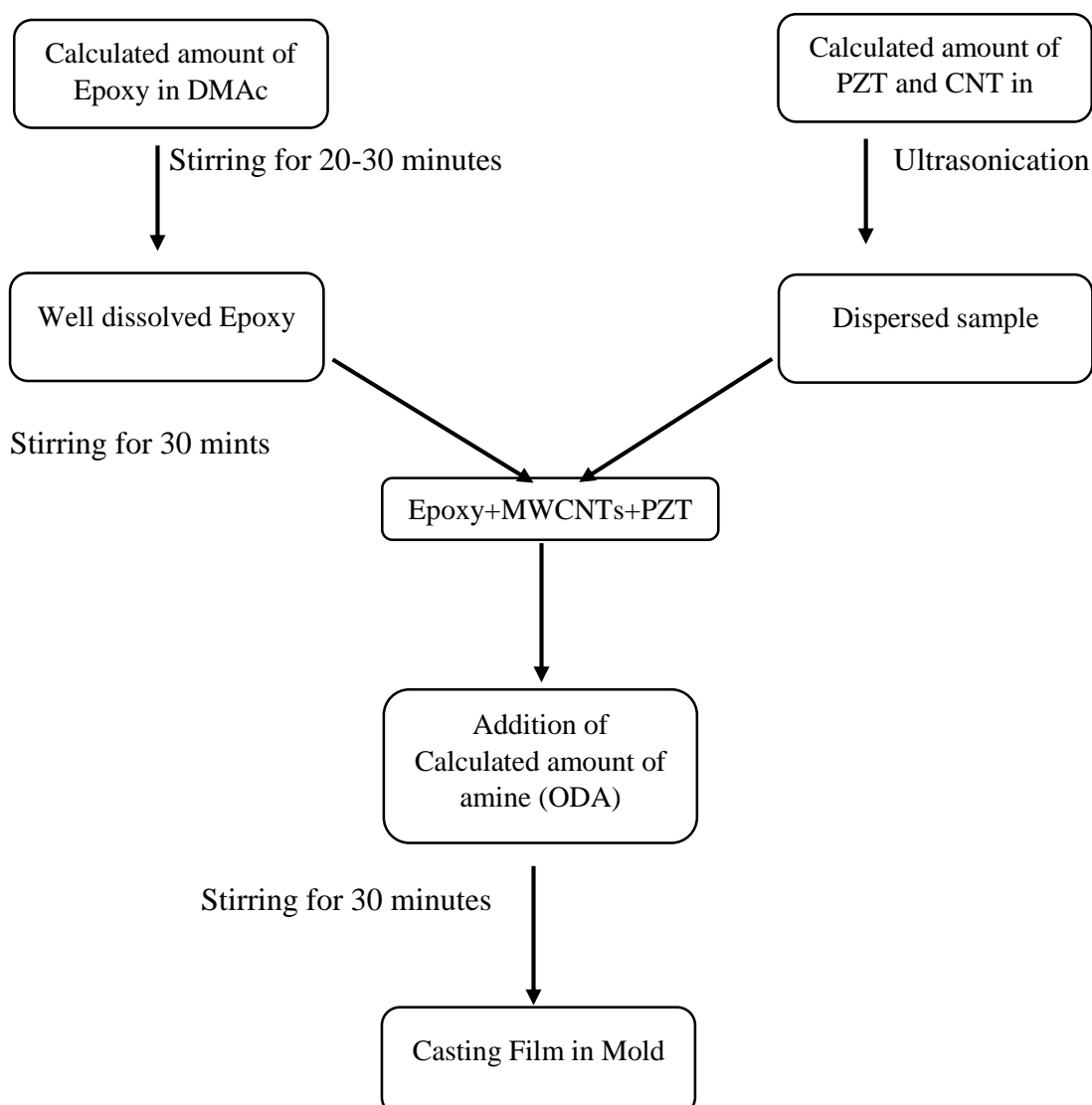
Figure 2.2: Steps of purification of CNTs.



2.6 STEP-2

2.6.1 Preparation of cured epoxy/MWCNT/PZT composite

A weighed amount of epoxy is dissolved into Dimethyl acetamide (DMAc) anhydrous and stirred for 20-30 minutes, on the other hand mixture of purified carbon nanotubes and PZT in same solvent were subjected to sonication, sonication was done for the dispersion of MWCNTs and PZT within solvent as both carbon nanotubes and PZT were non functionalized and to avoid any agglomeration formation sonication was done for 2-3 hours, when they are fully dispersed, the mixture is transferred into well dissolved epoxy and continued stirring for 30 minutes. In the last step, the curing agent i.e. ODA (4-4 Oxidianiline) was added and stirring was done for half an hour. The film was casted in a mold and solvent was evaporated by heating at 50 °C for 36 hours. Curing of epoxy was done for 4 hours at 80 °C and post curing at 120 °C and the solid epoxy/composite film was obtained.



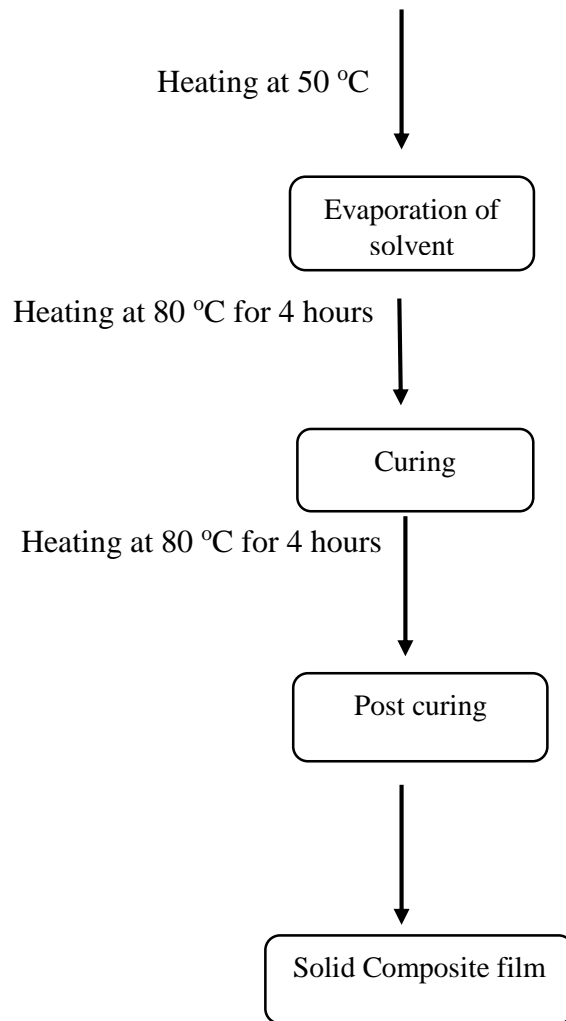


Figure 2.3: Scheme of preparation of composites.

2.7 Characterization of composites

Testometric universal testing machine (M500-30CT), as per ASTM standard D-882 was used for investigating mechanical properties of Epoxy/CNT/PZT composites.

X-ray Diffractometer, Model 3040/60 X'Pert PRO was used to record the XRD spectra. The XRD analysis of cured samples was carried out in form of films of composites and pure PZT powder, MWCNTs with scan-rate of 0.04 and 2θ values ranging from 0-50°.

Perkin Elmer's TGA 7 was used for thermogravimetric analysis at heating rate of 20°C/minute from ambient temperature to 600°C under nitrogen atmosphere.

An Agilent-4294A impedance/gain phase analyzer was used to determine Electrical conductivities of the composites with a voltage amplitude of 0.5-VAC at a frequency of 1 MHz.

Composites with different compositions were prepared to investigate the different properties and the effect of changing the weight % of the fillers. Various experimental techniques were used to analyze the prepared composites. X-ray diffraction analysis was used to evaluate the dispersion of added fillers in the epoxy matrix. Differential scanning calorimetry (DSC) was used to evaluate the effect of CNTs and PZT on glass transition temperature of epoxy matrix. Thermal stability of the prepared samples was evaluated using thermogravimetric analysis (TGA). Mechanical properties of the samples were tested using a tensile testing and electrical properties were examined by measuring electrical conductivities of the composites using a source meter.

3.1 X-Ray Diffraction analysis (XRD)

X-ray diffraction analysis is one of the best tools to investigate structure of carbon nanotubes. This technique provides basic information of interlayer spacing between nanotube walls with the help of strong peak appearing in the XRD pattern. The structural changes that appear in XRD spectra after introducing CNT's in epoxy matrix can also be analyzed. XRD spectrum of PZT was also investigated, before introducing PZT into the system and after completely dispersed into the matrix system. The XRD patterns of pristine CNTs , PZT and epoxy/PZT/CNT composite film are shown in figure 3.1.

To evaluate the structural changes occurring, at first pristine multiwall carbon were subjected to XRD analysis. A sharp and intense peak appearing at about $2\theta = 26^\circ$, corresponds to (002) Bragg reflection plane having an interlayer spacing of 0.33 nm. Another comparatively broad peak was shown at about $2\theta = 45^\circ$ having Bragg reflection plane equal to (100) and interlayer spacing of 0.2 nm and is assigned to the reflection of graphite like structure (100). Peak at $2\theta = 26^\circ$ is the characteristic peak of MWCNTs which is known as Bragg peak and is produced by constructive interference

of various reflection planes as reported in literature [133]. XRD spectra of PZT shows one clear peak at $2\theta = 31^\circ$ and small peaks at $2\theta = 22^\circ, 38^\circ, 44^\circ$ & 55° . These peaks shows crystalline nature of PZT.

The XRD spectra of the composites reveals two clear peaks one at $2\theta = 26^\circ$ which is characteristic peak of carbon nanotubes the reduction in the peak intensity confirms the dispersion of CNTs in the matrix another peak at $2\theta = 30.5^\circ$ which is characteristic peak of PZT crystals the peak intensity is reduced when PZT is incorporated as a filler in the epoxy matrix which reveals that PZT is dispersed in the matrix [134].

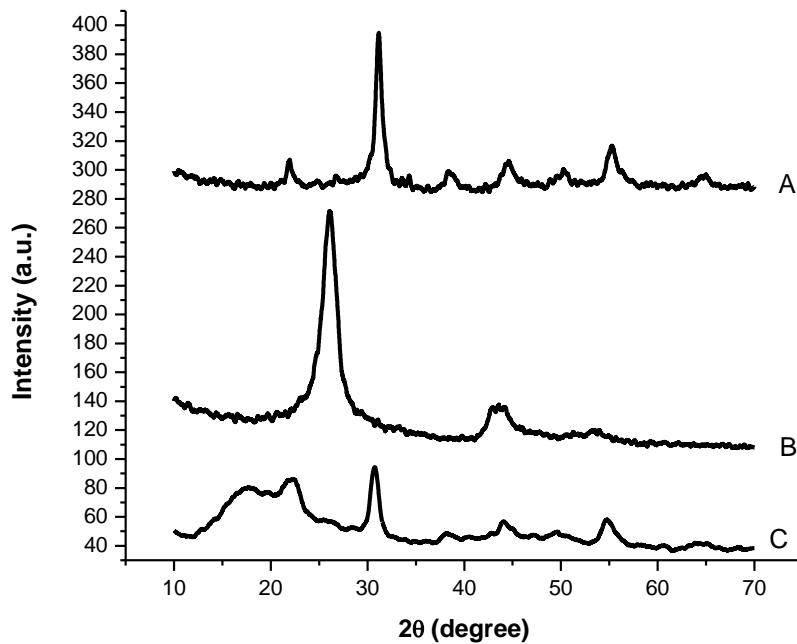


Figure 3.1: Combined XRD pattern of (A) PZT, (B) MWCNTs and (C) epoxy/CNT/PZT composite.

3.2 THERMAL ANALYSIS

3.2.1 Differential scanning calorimetry (DSC)

Differential scanning calorimetry is one of the best tools to study the cure reaction, cure kinetics and to evaluate glass transition of epoxy [135]. The polymers undergo a rapid loss of modulus on glass transition temperatures. Therefore, for best utilization of a polymer, knowledge of its thermal behavior also plays a significant role. In present work differential scanning calorimetry (DSC) was used to evaluate the glass transition temperature (T_g) of epoxy samples cured with ODA. The T_g is a very important parameter of thermal properties for the epoxy based composites. In most cases, epoxy based composites are only used well at the temperature below T_g therefore, identification of the mechanisms responsible for T_g changes and prediction of T_g depression are critical for the engineering design and the application of such composites [136].

Some selective samples were chosen to study the effect of filler on glass transition temperature of cured epoxy. All DSC thermograms were obtained as heating cooling heating pattern to confirm the transition of glassy to rubbery state from 50 °C to 250 °C at 10 °C/min heating rate under nitrogen atmosphere. These thermograms were used to calculate glass transition temperature (T_g) of uncured (for neat epoxy) and cured samples.

Glass transition temperature of cured epoxy is highly affected by the stoichiometry of the cure reaction i.e. mole ratio of curing agent or hardener. Epoxide groups undergo homo polymerization during the curing reaction; hence once the curing agent is completely consumed the remaining epoxide rings react with each other to develop a 3-D network [137]. The extent of cross-linking is also one of the main reasons for change in T_g . Moreover reaction temperature also plays an important role to alter the temperature of this transition.

An evident transition in temperature can be observed at -8 °C, which is glass transition temperature of uncured epoxy resin. Figure 3.2 represents epoxy cured with ODA sample. The glass transition temperature of the resin was increased to 67 °C from uncured to cured state. This confirms the completion of curing reaction and formation of an extensive three dimensional cross-linking network due to curing reaction.

Addition of multiwalled carbon nanotubes does not cause any major change in the glass transition temperature of the composite except a slight decrease in glass transition temperature.

However, addition of PZT causes increase in glass transition temperature this is because PZT is brittle in nature having high thermal stability and thus incorporation of PZT into epoxy matrix increases brittleness of the epoxy matrix as evident in increasing glass transition temperature [129], which is shown in (Figure 3.4-Figure 3.9). Carbon nanotubes causes very little decrease in glass transition temperature because incorporation of carbon nanotubes decreases cross linking density of the epoxy matrix by increasing elasticity of the epoxy matrix and decreasing brittleness. Table 3.1 shows the values of glass transition temperature of all samples, it is shown that the cured epoxy without fillers bears higher glass transition temperature than all other samples containing different CNTs and PZT.

Table 3.1: Calculated Glass transition temperature (T_g) of all the composites.

S.No.	Sample	T_g (°C)
1	Uncured epoxy	-8
2	E-0-0	67
3	E-1-0	61
4	E-1-10	62
5	E-1-20	64
6	E-1-30	65
7	E-1.5-10	62
8	E-1.5-20	63
9	E-1.5-30	65
10	E-2-10	58
11	E-2-20	59
12	E-2-30	61

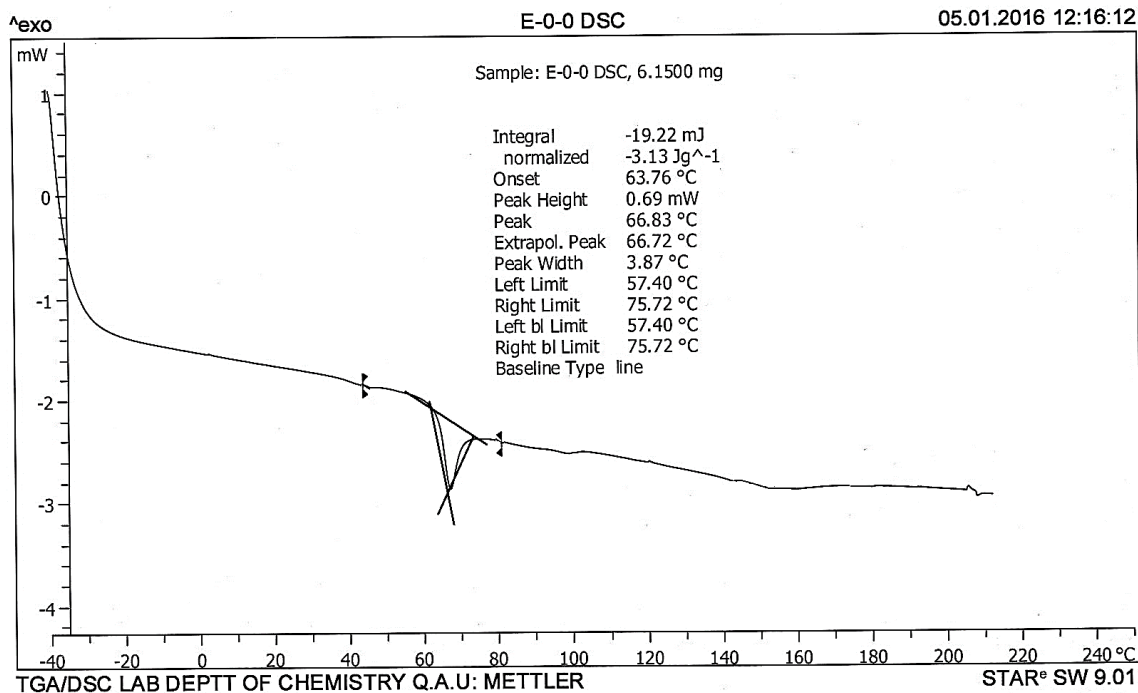


Figure 3.2: DSC thermogram of ODA cured epoxy.

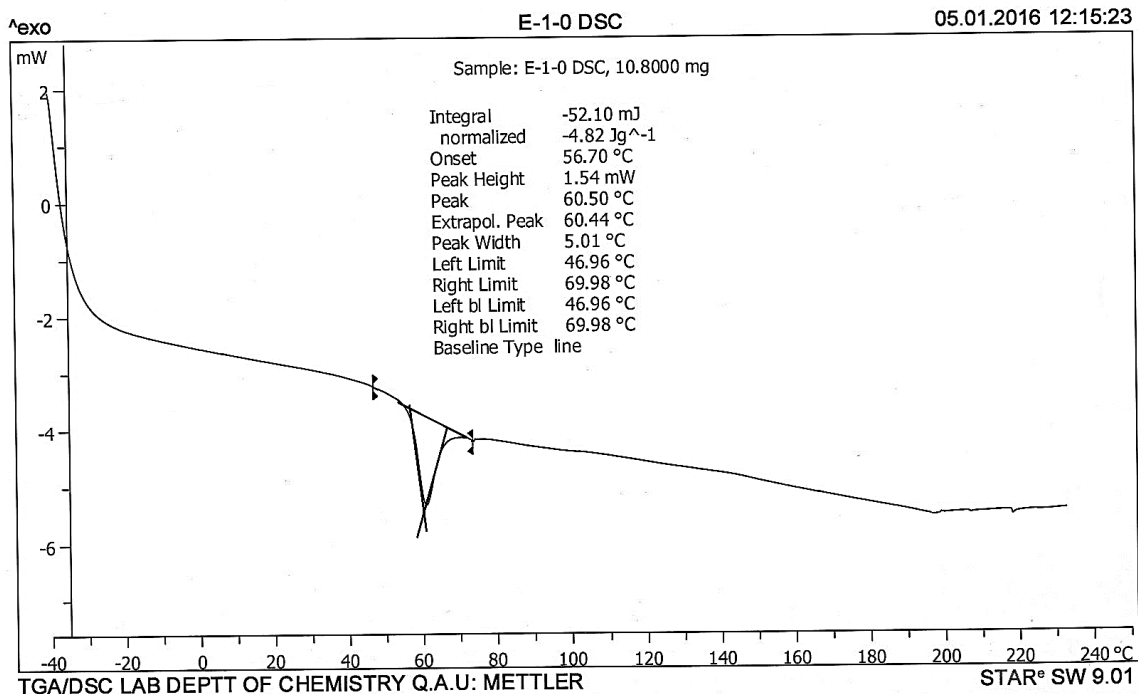


Figure 3.3: DSC thermogram of epoxy/CNT composite E-0-0.

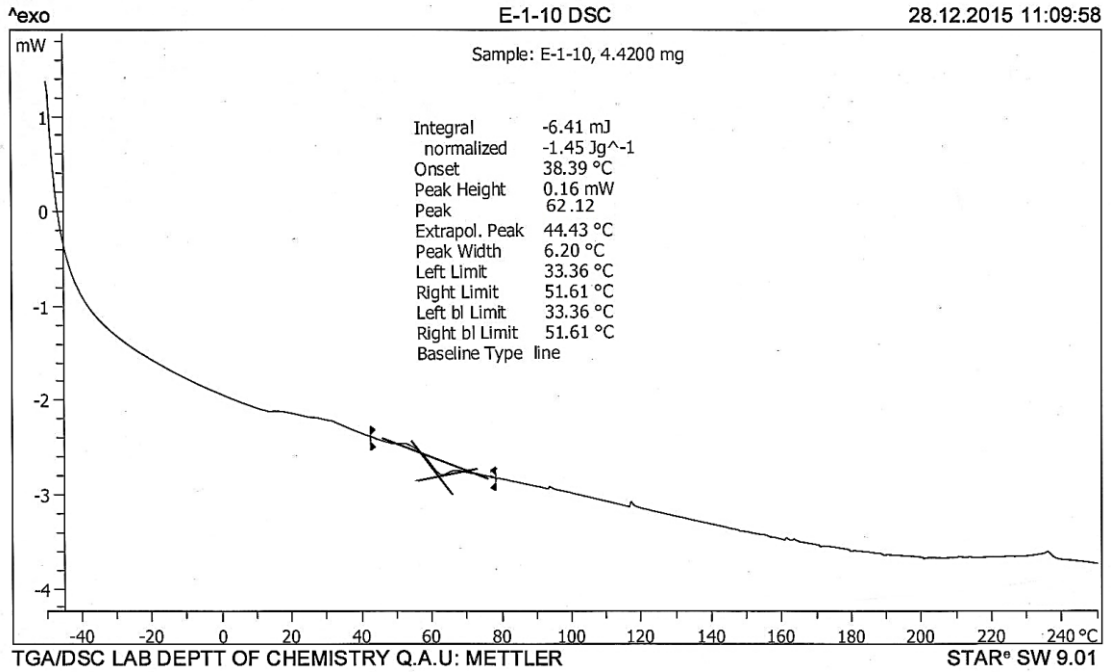


Figure 3.4: DSC thermogram of epoxy/CNT/PZT composite E-1-10.

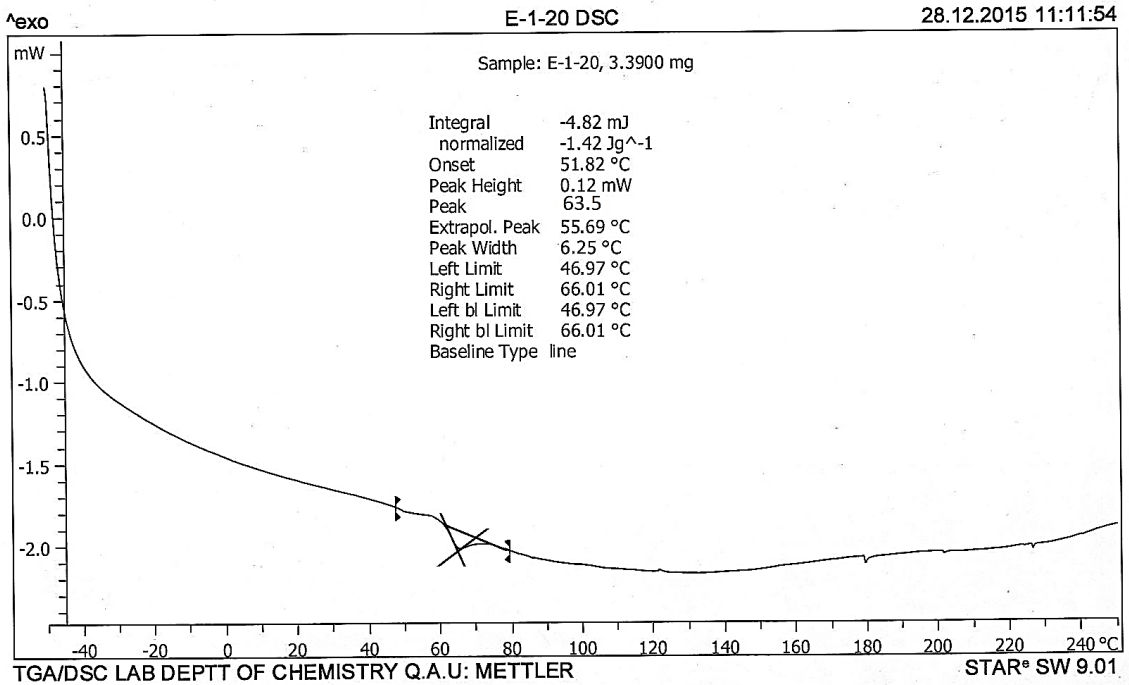


Figure 3.5: DSC thermogram of epoxy/CNT/PZT composite E-1-20.

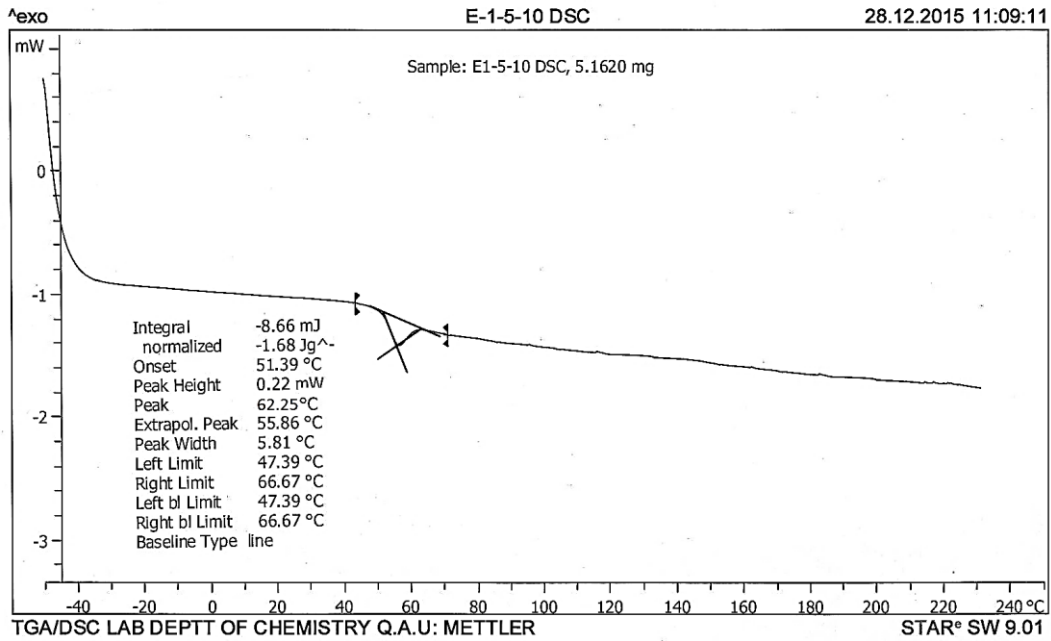


Figure 3.6: DSC thermogram of epoxy/CNT/PZT composite E-1.5-10.

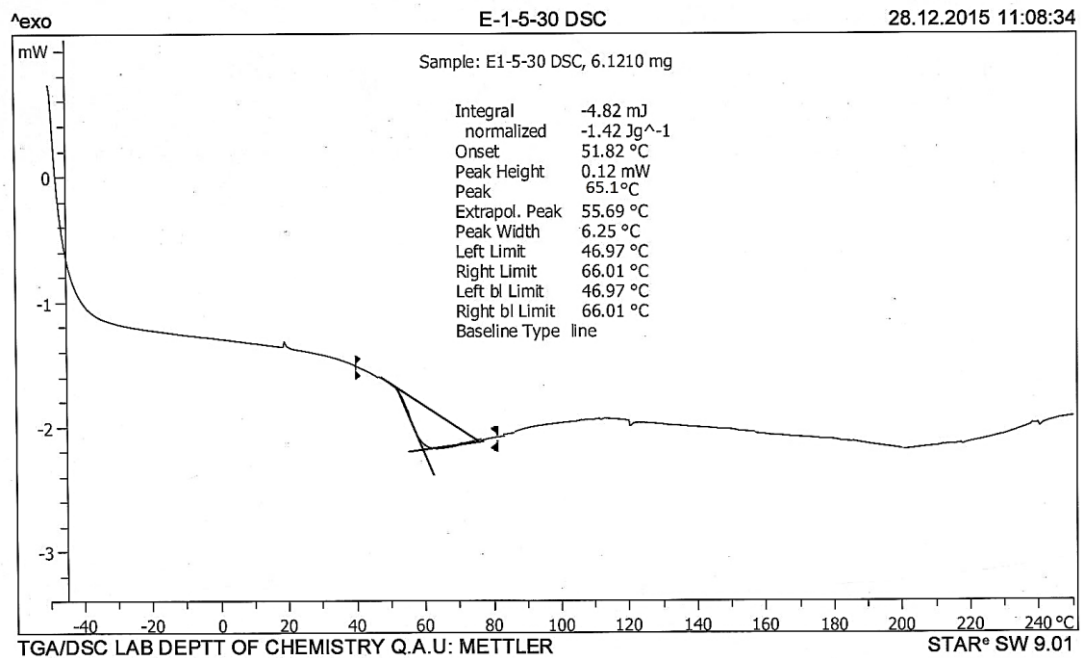


Figure 3.7: DSC thermogram of epoxy/CNT/PZT composite E-1.5-30.

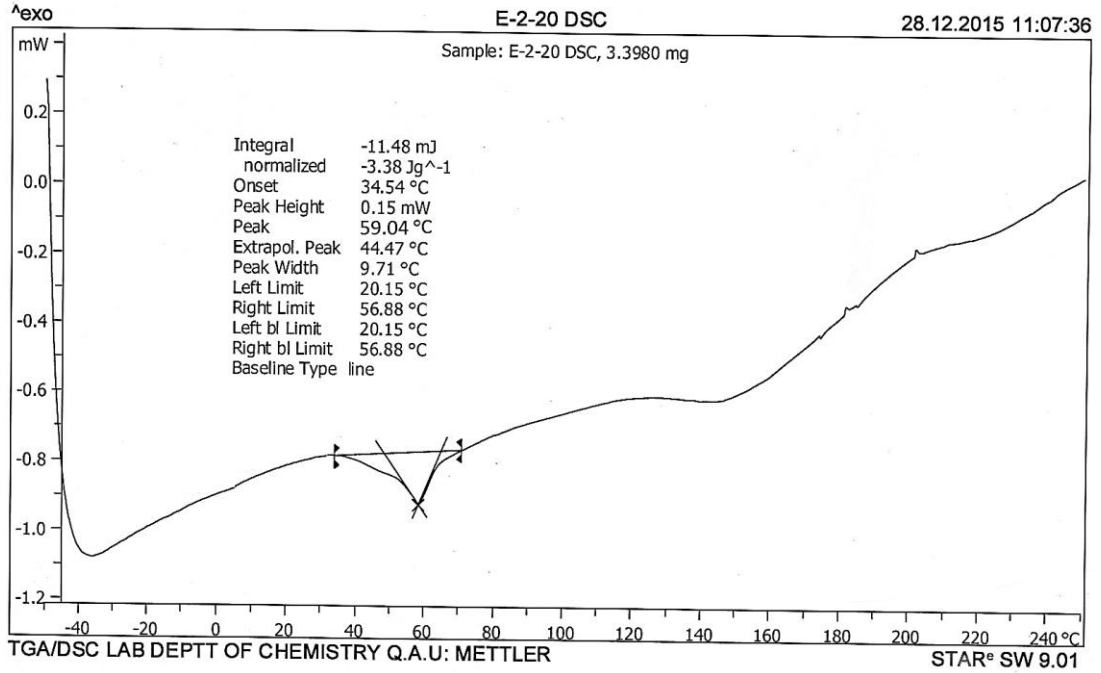


Figure 3.8: DSC thermogram of epoxy/CNT/PZT composite E-2-20.

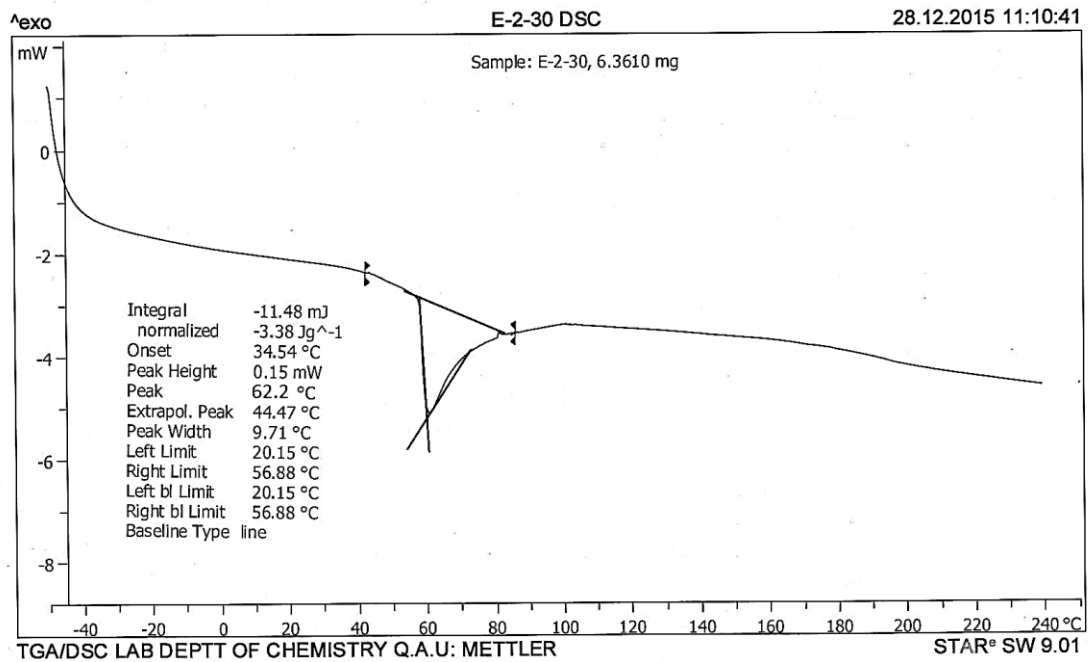


Figure 3.9: DSC thermogram of epoxy/CNT/PZT composite E-2-30.

3.2.2 Thermogravimetric analysis (TGA)

Thermogravimetric analysis is frequently used to evaluate thermal stability of materials and decomposition of polymers at different temperatures [138]. Some selected samples were used to study the thermal stability of cured resin from room temperature to 600 °C at the rate of 10 °C/minute in nitrogen environment and weight loss of each sample were recorded with increase in temperature.

Different parameters were calculated using thermograms, such as temperature at 10% weight loss (T_{10}), temperature at which onset of degradation starts (T_{onset}), temperature corresponding to maximum weight loss occurs (T_{max}) and char yield remaining at the completion of degradation process. The relative thermal stability of the cured resin was evaluated by comparing the T_{onset} , T_{10} , T_{max} and char yield and TGA data obtained from thermograms is given in Table.3.2. It can be observed from given thermograms that first there is a step where little degradation starts and in second step a proper degradation of cured sample starts. 10 % weight loss of all the samples lie between 250-350 °C whereas maximum degradation occurs between 350-450 °C this temperature is very important for the composites.

It can be obtained from the TGA thermograms that by incorporation of fillers in the epoxy matrix i.e. CNTs and PZT the maximum degradation temperature of the epoxy matrix or T_{max} increases, which shows increased thermal stability of the composites. This improvement mainly comes from the enhanced interaction between epoxy matrix and fillers [139]. Furthermore, it may also be assumed that the thermal stability of organic materials can be improved by introducing inorganic components on the basis of the fact that these materials have inherently good thermal stability [140].

All the samples show no significant weight loss up to 100 °C, which confirms that samples were completely anhydrous and the first step to degradation starts after 200 °C. In first step of transition for all the samples the weight loss is not more than 15 %, which suggests that the transition is because of evaporation of solvent molecules or some volatile organic molecules present in the sample in the form of impurities.

Figure 3.10 represents TGA thermograms of cured epoxy, CNT incorporated epoxy and PZT incorporated epoxy it can be seen from the curves that presence of these fillers improves thermal stability by shifting T_{max} at higher temperature and char yield also increases by incorporation of the fillers.

Figure 3.11 represents TGA thermograms of the composites in which effect of increasing CNT loading is shown by keeping constant PZT. This graph clearly shows that by increasing CNT loading improves thermal stability.

Figure 3.12 represents combined thermograms of different PZT weight percentage, PZT due to its highly brittle nature and improved thermal stability plays important role in the enhancement of thermal properties of the epoxy matrix. Various parameters, calculated from TGA thermograms are listed below in table 3.2.

Table 3.2: TGA data showing various parameters calculated from thermograms.

S.No.	Sample	T₁₀ (°C)	T_{onset} (°C)	T_{offset} (°C)	T_{max.} (°C)	Char Yield (%)
1	E-0-0	267.1	365.77	441.79	336.76	14.7
2	E-1-0	241.3	363.02	428.39	401.11	20.5
3	E-1-10	255.1	333.22	460.71	400.32	25.5
4	E-1-20	309.2	334.65	454.59	399.77	40.3
5	E-1.5-10	369.5	337.04	443.24	389.82	27.7
6	E-1.5-30	248.4	329.25	443.25	396.50	38.2
7	E-2-10	232.7	357.62	423.33	392.62	19.1
8	E-2-20	340.5	348.59	432.93	294.26	29.3

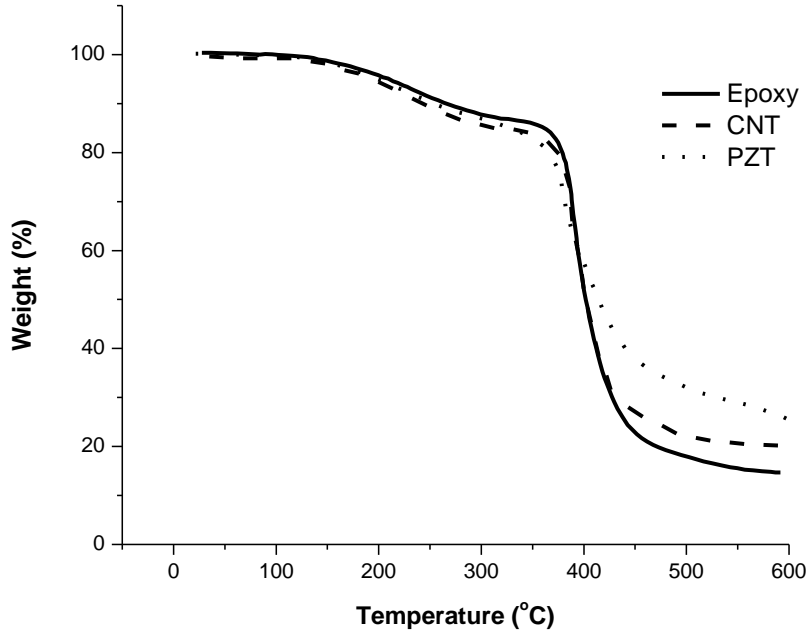


Figure 3.10: TGA thermograms of cured epoxy, epoxy/CNT composite and epoxy/CNT/PZT composite.

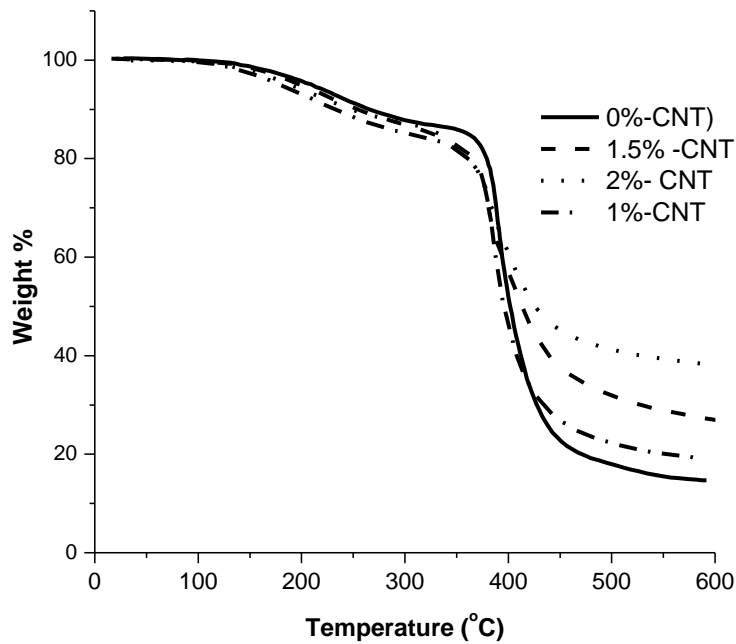


Figure 3.11: Combined TGA thermograms of composites by varying CNT loading.

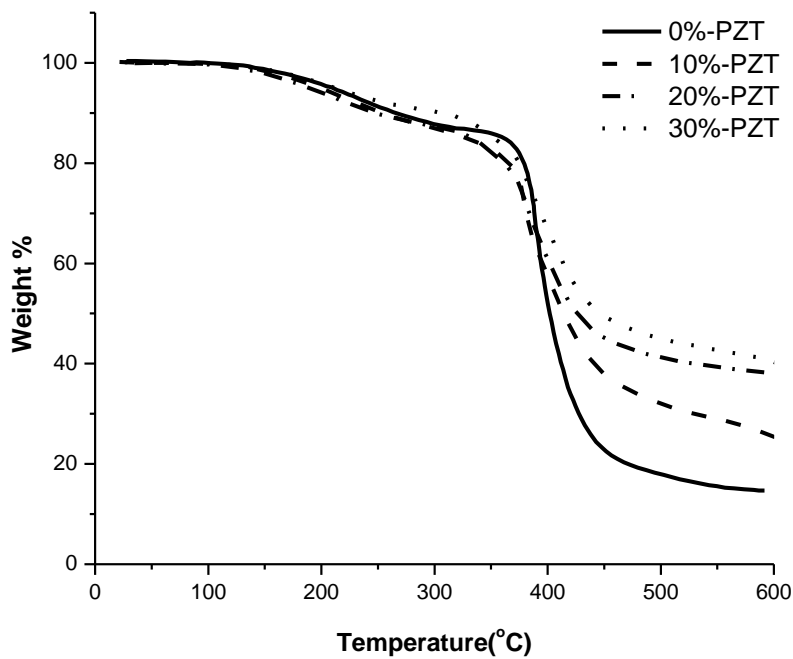


Figure 3.12: Combined TGA thermograms of epoxy/CNT/PZT composites of different PZT loading.

3.2.3 Tensile testing

Tensile testing is also known as “tension testing”. Tensile tests measure the force required to break a sample specimen and the extent to which the specimen stretches or elongates to that breaking point. Mechanical properties such as stress at break, elongation, modulus, and toughness of the cured epoxy films were determined by stretching the rectangular strips having dimensions of $40 \times 7 \times 0.05 \text{ mm}^3$ at a crosshead speed of 2 mm/min using testometric universal testing machine, according to ASTM D-882. The results reported are averaged from at least three measurements per sample.

A stress versus strain curve is obtained which is used to determine tensile properties like Young’s modulus, stress at break, strain at break and toughness. A typical Stress strain curve and properties obtain from this curve are shown in Figure 3.13

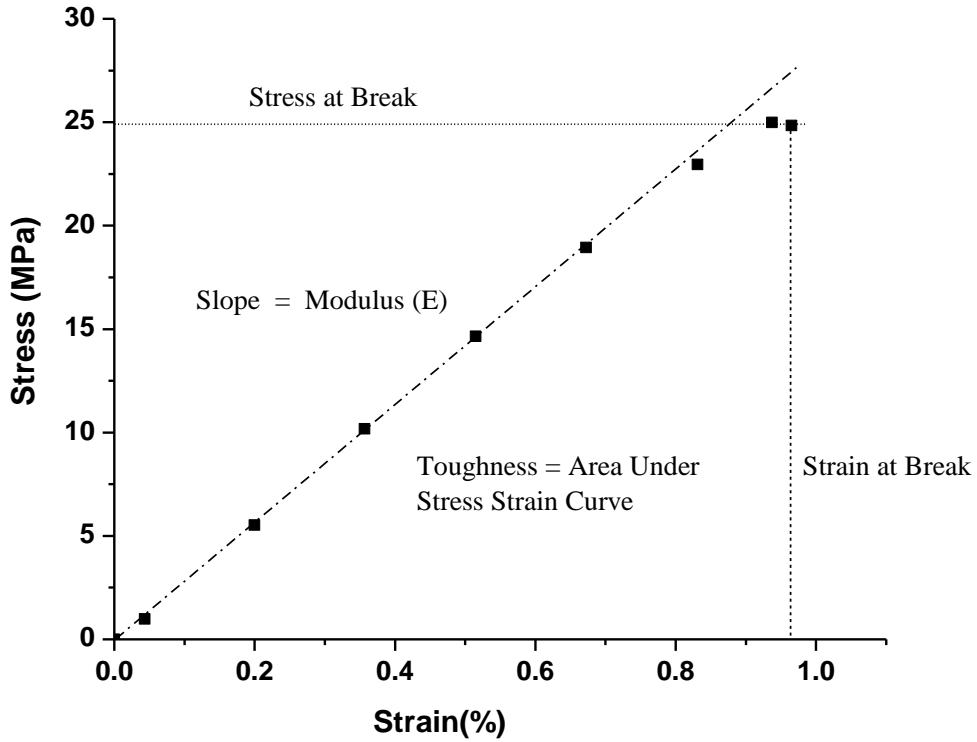


Figure 3.13: Typical stress-strain curve for polymers.

3.2.3.1 Stress-strain analysis of CNT and PZT incorporated composites

Stress-strain curves of composites are shown in figures 3.14-3.25, it is observed that the initial stress-strain curve is linear and the slope of that line represents brittle behavior of the composites higher the value of the slope greater will be the brittleness, various parameters were calculated using these stress-strain curves such as toughness, Young's modulus, stress at break and ultimate tensile strength values are calculated.

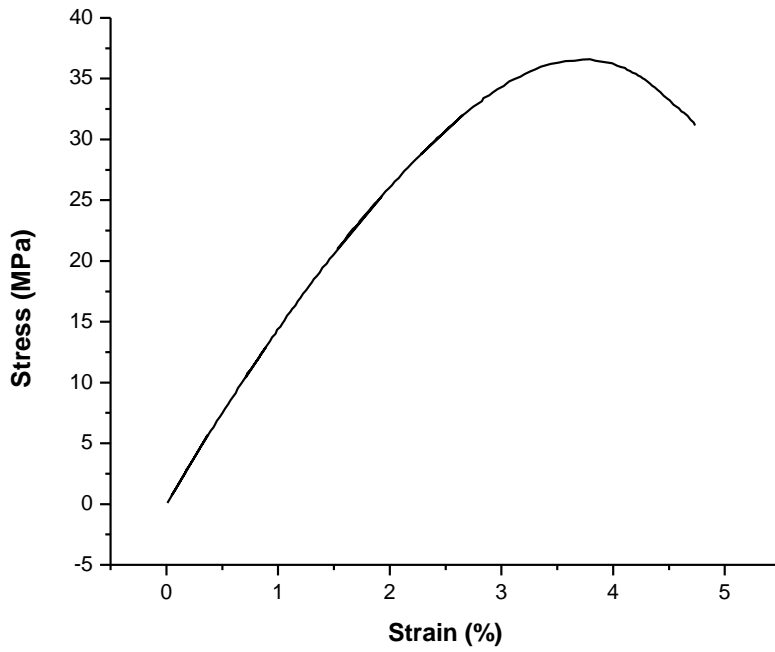


Figure 3.14: Stress-strain curve of cured epoxy.

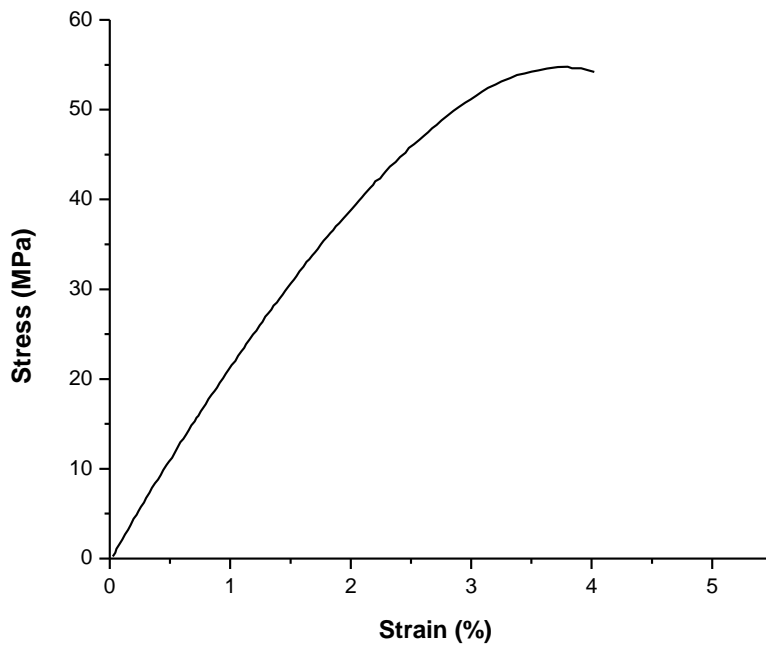


Figure 3.15: Stress-strain curve of epoxy/CNT composite E-1-0.

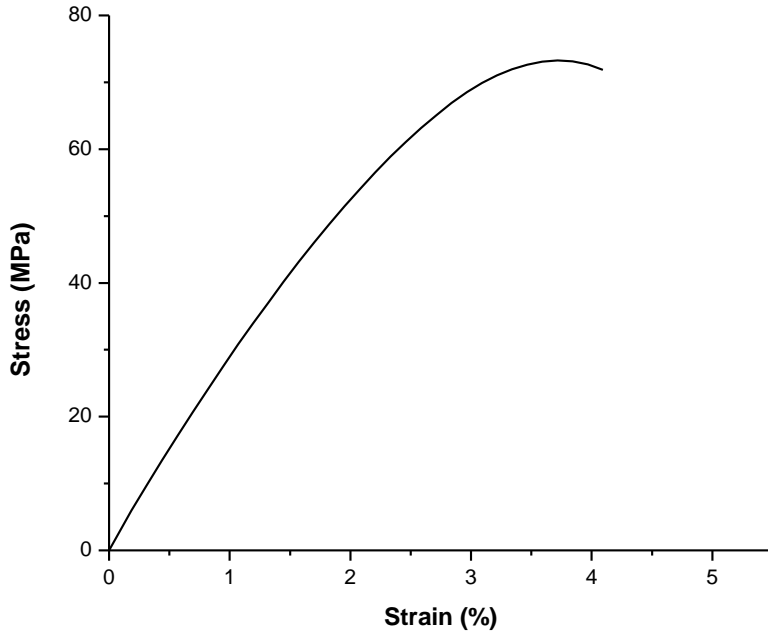


Figure 3.16: Stress-strain curve of epoxy/CNT/PZT composite E-1-10.

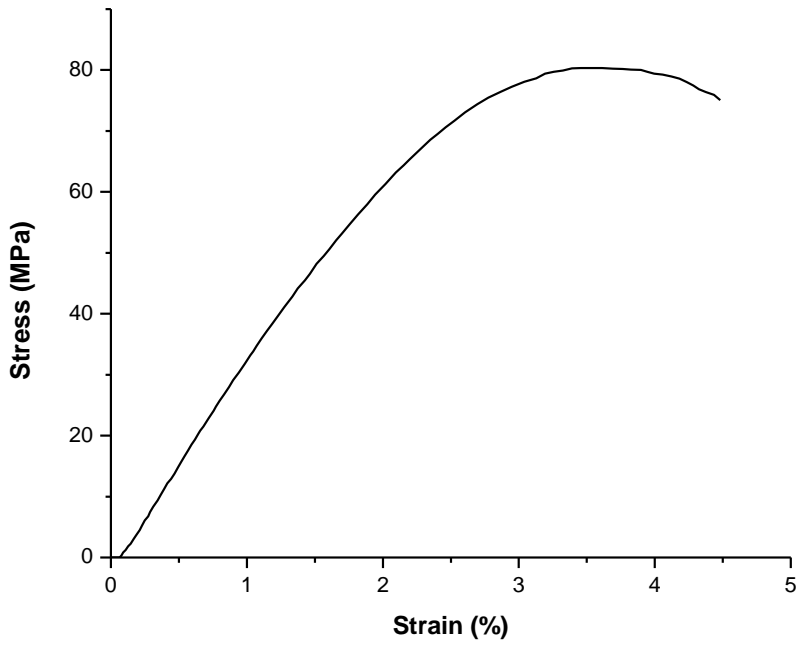


Figure 3.17: Stress-strain curve of epoxy/CNT/PZT composite E-1-20.

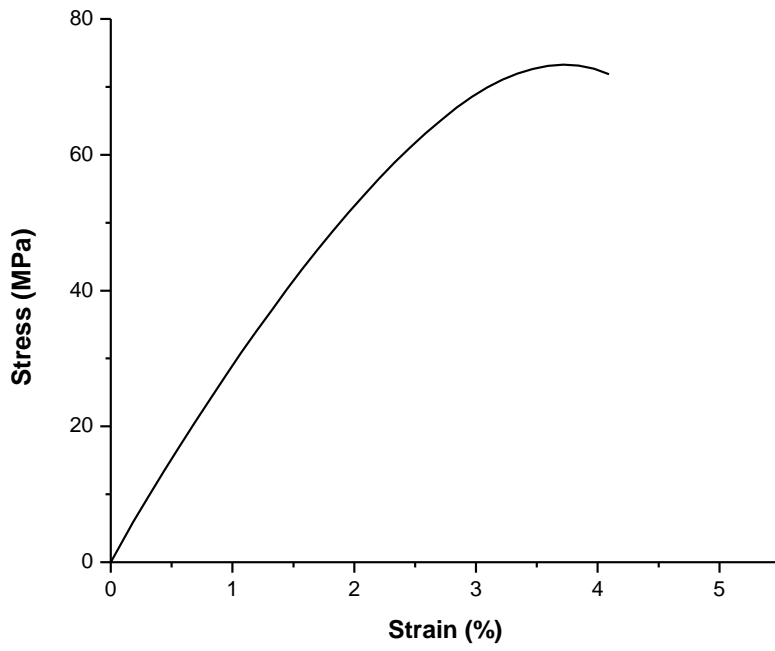


Figure 3.18: Stress-strain curve of epoxy/CNT/PZT composite E-1-30.

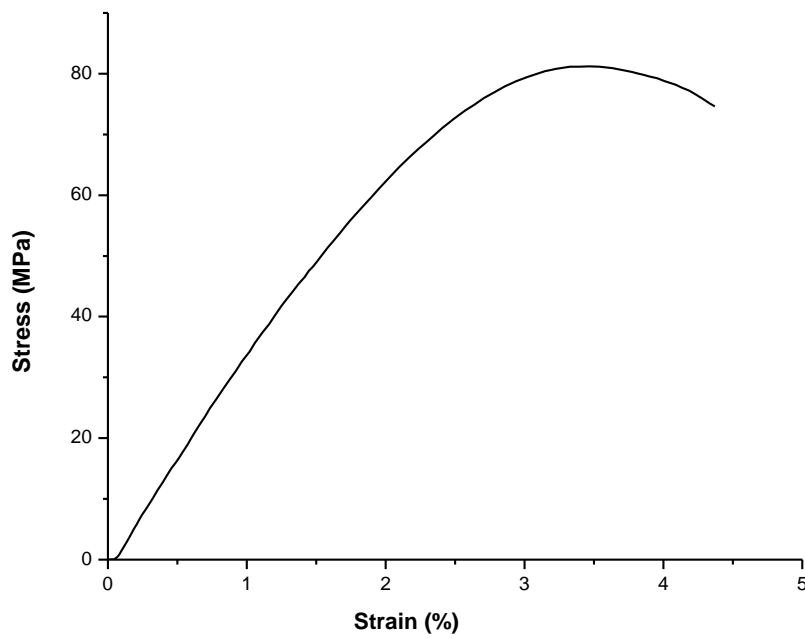


Figure 3.19: Stress-strain curve of epoxy/CNT/PZT composite E-1.5-10.

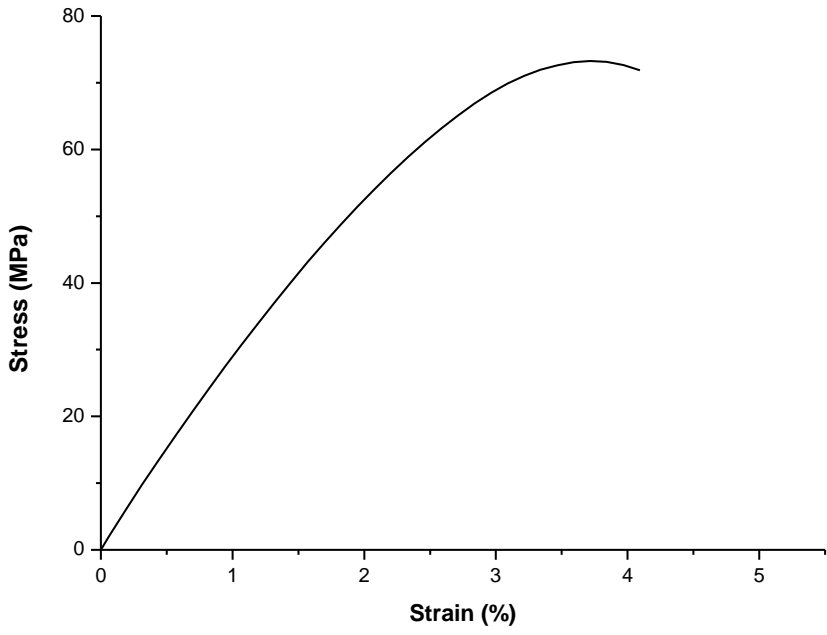


Figure 3.20: Stress-strain curve of epoxy/CNT/PZT composite E-1.5-20.

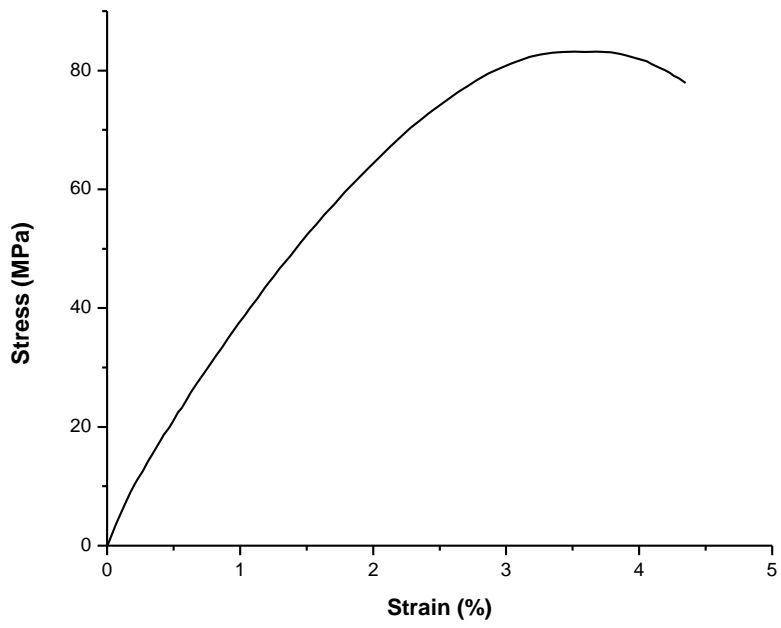


Figure 3.21: Stress-strain curve of epoxy/CNT/PZT composite E-1.5-30.

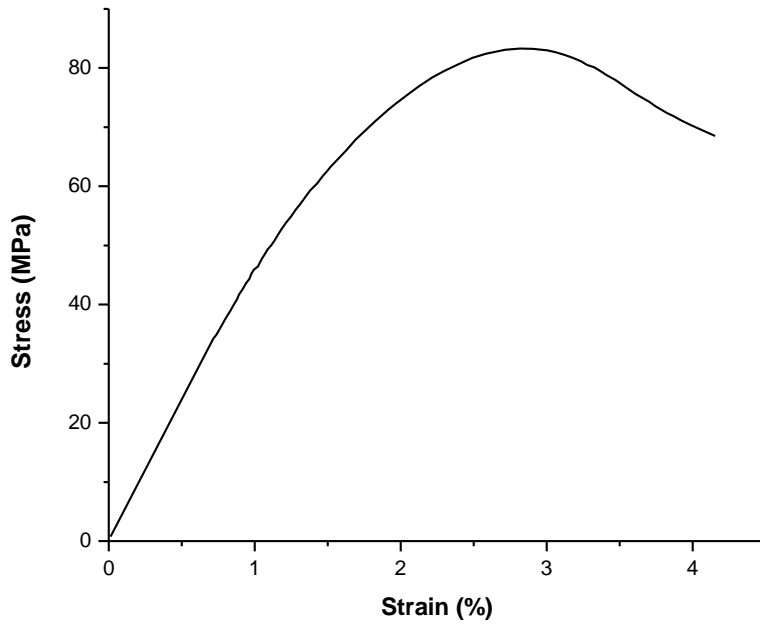


Figure 3.22: Stress-strain curve of epoxy/CNT/PZT composite E-2-10.

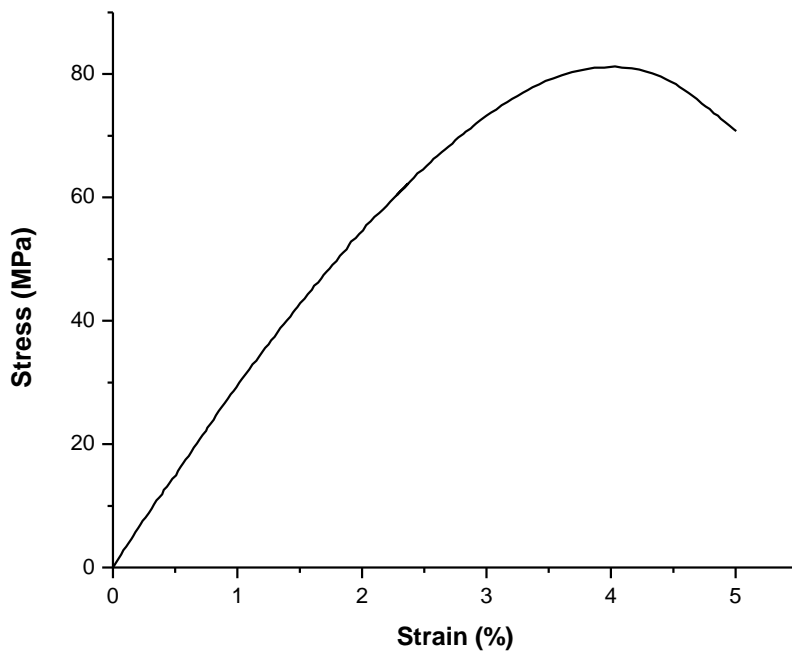


Figure 3.23: Stress-strain curve of epoxy/CNT/PZT composite E-2-20.

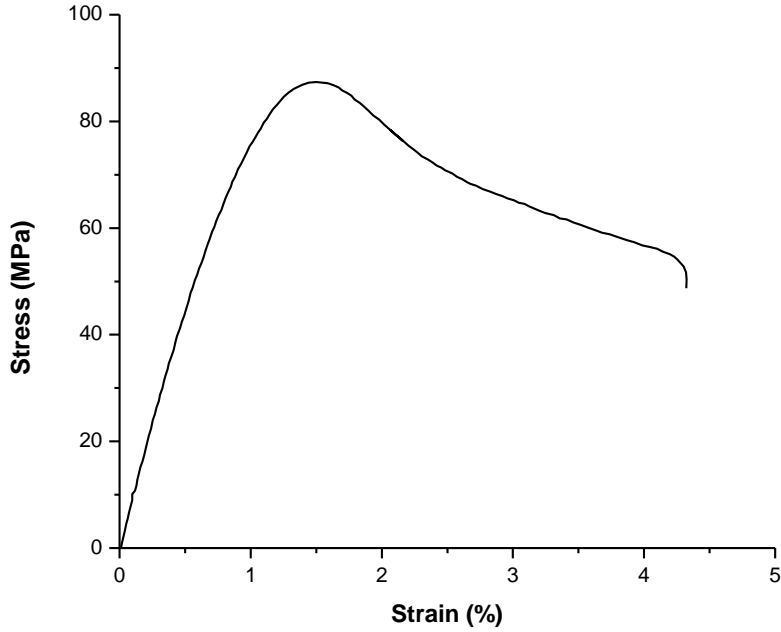


Figure 3.24: Stress-strain curve of epoxy/CNT/PZT composite E-2-30.

3.2.3.2 Toughness

Toughness is the ability of a material to absorb energy for deformation without fracturing. In other words it is the amount of energy per unit volume that a material can absorb before rupturing. Elastic materials have more toughness than brittle materials. Toughness is inverse of brittleness. It is calculated from area under the curve obtained from integrating over stress-strain curve. Toughness values for all composites is given in the table 3.3. It is shown from the values that cured epoxy is brittle and have little toughness by incorporating carbon nanotubes the toughness of the epoxy matrix increases [141], while PZT increases brittleness in the composites because PZT is brittle in nature.

The objective of the work was to decrease the brittle nature of the PZT crystals by incorporating such type of filler which enhances the toughness. Epoxy matrix have poor mechanical properties it is seen that the addition of fillers enhances the mechanical properties of the epoxy matrix, the composites have excellent mechanical properties than the cured epoxy. Figure 3.25 shows the graph in which toughness of the composites is plotted against CNT loading, it is seen that by increasing CNT loading toughness of the composites increases. Figure 3.26 shows toughness of the composites by varying the percentage of PZT it is seen that the composites having low amount of

PZT have low Toughness, by increasing the PZT loading toughness of the composites is decreased [142].

Table 3.3: Values of toughness calculated for all composites.

S.No.	Sample	Toughness(Mpa)
1	E-0-0	46
2	E-1-0	263.12
3	E-1-10	246.80
4	E-1-20	207.10
5	E-1-30	182.30
6	E-1.5-10	273.0
7	E-1.5-20	250.55
8	E-1.5-30	213.22
9	E-2-10	307.7
10	E-2-20	246.8
11	E-2-30	211.86

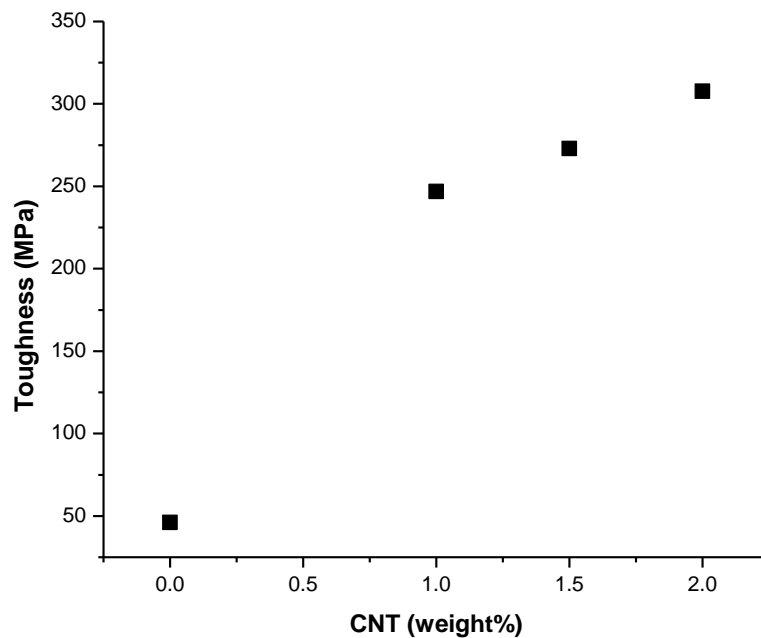


Figure 3.25: Toughness of composites with increasing CNTs loading.

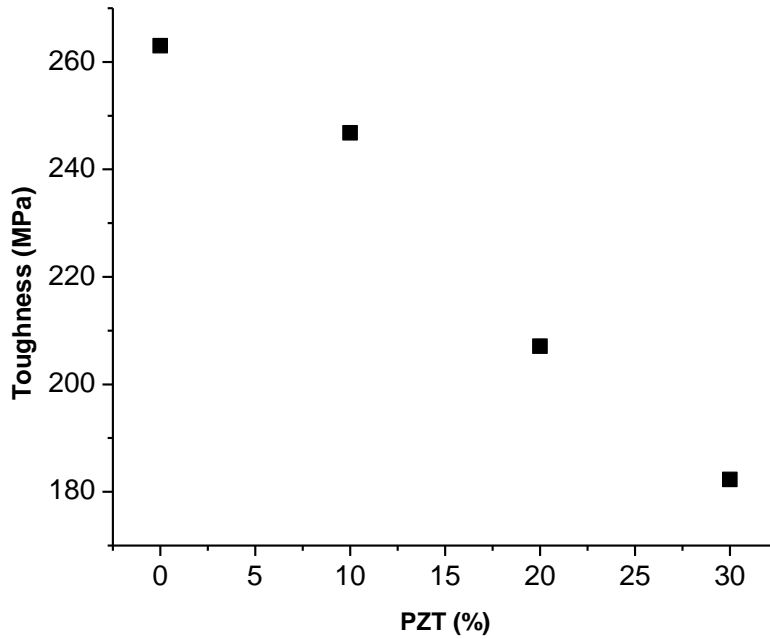


Figure 3.26: Toughness of composites with increasing PZT loading.

3.2.3.3 Young's modulus

Young's modulus is the ratio of stress to strain, it is also called modulus of elasticity. It is the materials resistance to deformation when a stress is applied. It represents stiffness of the material higher the value of Young's modulus more stiffness will be the material. Stiffness is the amount of mechanical force needed to deform a material that is by compression, bending, or extension. Stiffer the material the more force is needed to deform the material of same length. It is shown by "Y" it is given by

$$Y = \frac{\text{Stress}}{\text{Strain}} = \frac{F/A}{L/\Delta L} = \frac{FL}{A\Delta L}$$

It is measured in Pascal. It is calculated from the stress strain curve by using initial slope method. The stress strain curve is linear initially by calculating the slope of that line Young's modulus is calculated. Table. 3.4 shows the values of Young's modulus for all composites it is seen that by incorporation of fillers the young's modulus of the epoxy matrix is increased [143]. Figure 3.27 represents effect of CNT loading on the young's modulus of composites keeping PZT constant it is seen that Young's modulus is increased by increasing the CNT loading in the composites which shows improvement in the mechanical strength of epoxy matrix by introducing CNTs in the matrix [144]. Figure 3.28 shows Young's modulus by varying the PZT loading, PZT also increases the stiffness of the composites by increasing the young's modulus [145].

Table 3.4: Calculated values of Young's modulus for all composites.

S.No.	Sample	Young's modulus(Mpa)
1	E-0-0	19.4
2	E-1-0	26.21
3	E-1-10	28.43
4	E-1-20	28.86
5	E-1-30	29.20
6	E-1.5-10	32.69
7	E-1.5-20	31.65
8	E-1.5-30	34.81
9	E-2-10	36.39
10	E-2-20	27.33
11	E-2-30	38.27

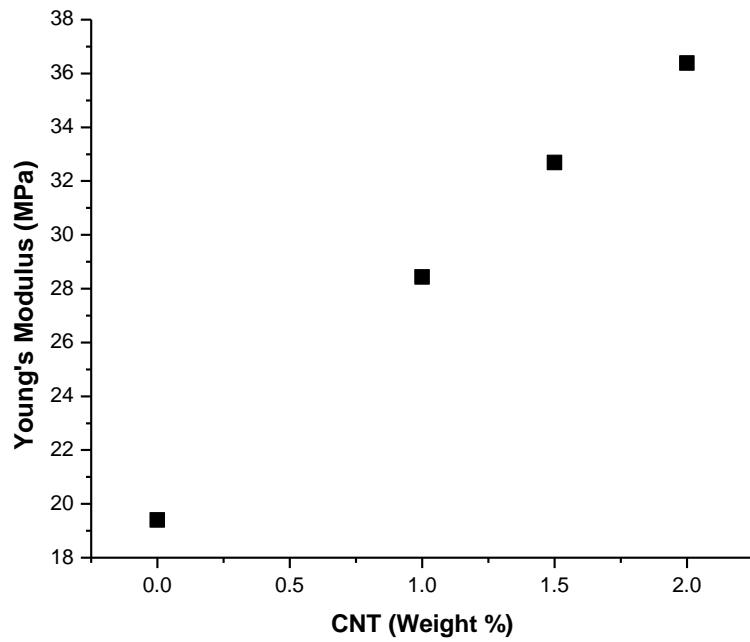


Figure 3.27: Effect of CNT loading on Young's modulus of composites.

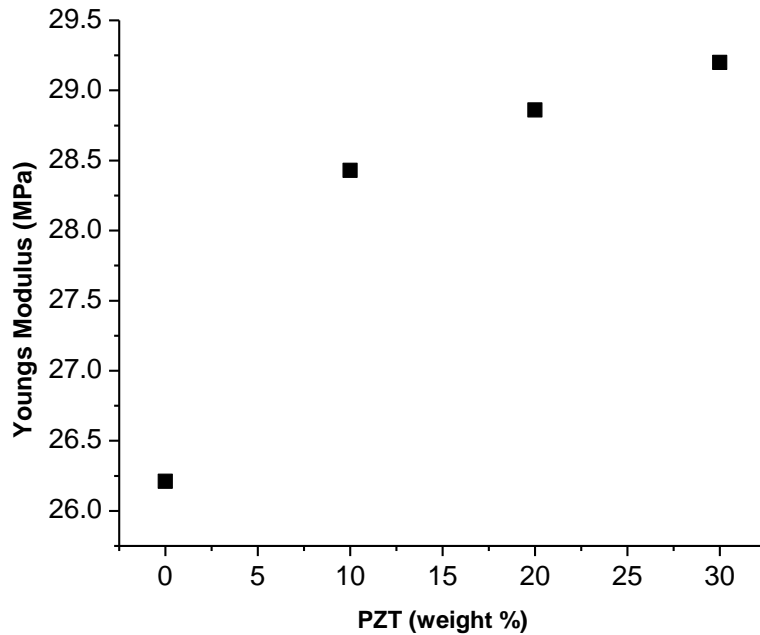


Figure 3.28: Effect of PZT loading on Young's modulus calculated for different composites.

3.2.3.4 Stress at break

It is the amount of stress at breaking point or the maximum stress at which a material is teared apart. It is calculated from stress strain curve the point at which the curve falls shows tensile stress at break in other words it is the amount of force needed to break the material apart. Table 3.5 shows the values of tensile stress at break calculated for all composites. It is observed that cured epoxy without the addition of fillers break quickly due to its highly brittle nature, by introducing fillers in the epoxy matrix, stress at break increased which shows enhanced mechanical strength of the matrix by addition of the fillers, this is because of incorporation of fillers cross linking density of the epoxy which results in increase in stress at break, effect of CNTs and PZT is shown in figures 3.29 & 3.30 respectively which shows that by increasing the amount of both fillers in the epoxy matrix increases the stress at break values for the composites.

Table 3.5: Calculated values of stress at break for different composites.

S.No.	Sample	Stress at break (MPa)
1	E-0-0	26.0
2	E-1-0	45.0
3	E-1-10	62.5
4	E-1-20	65.4
5	E-1-30	67.3
6	E-1.5-10	67.3
7	E-1.5-20	64.2
8	E-1.5-30	72.9
9	E-2-10	75.6
10	E-2-20	62.9
11	E-2-30	79.1

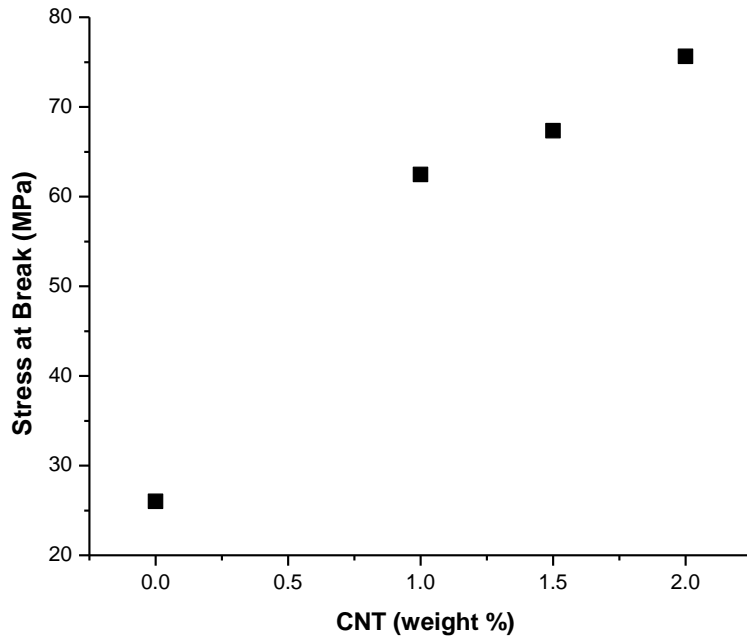


Figure 3.29: Values of stress at break for different composites against CNT loading.

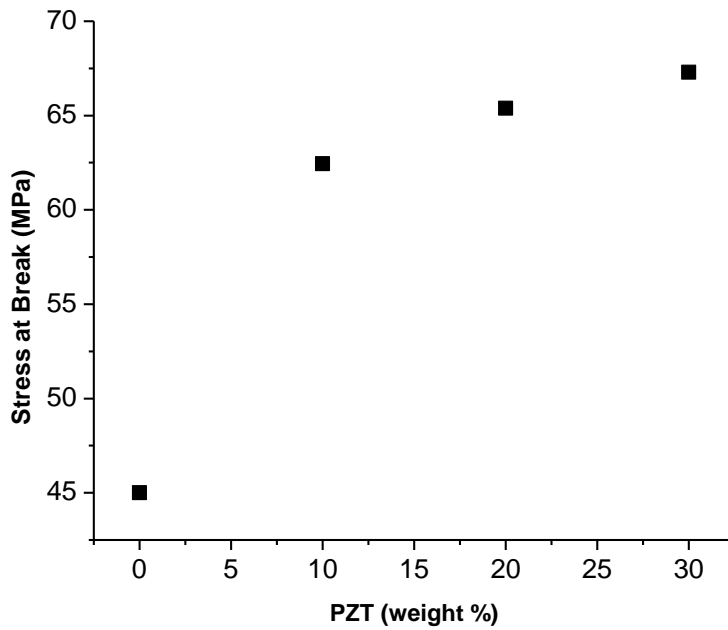


Figure 3.30: Calculated values of stress at break for different composites against PZT loading.

3.2.3.5 Ultimate tensile strength

Ultimate tensile strength is referred to maximum stress a material can bear before breaking. It is very important property of the composites, ultimate tensile strength is a measure of how much material is resistant towards applied stress. It is also called tensile strength cured epoxy has low ultimate tensile strength and by addition of fillers increase in the tensile strength. Table 3.6 shows values of the Tensile strength calculated for all the samples. Figures 3.31 & 3.32 shows effect of CNTs and PZT on the tensile strength of the epoxy matrix, it is observed clearly that by increasing the amount of CNT and PZT tensile strength of the composites also increases [129, 146].

Table 3.6: Calculated values of ultimate tensile stress for all composites.

S.No.	Sample	Tensile Strength (MPa)
1	E-0-0	37.12
2	E-1-0	62.0
3	E-1-10	73.28
4	E-1-20	75.36
5	E-1-30	77.0
6	E-1.5-10	79.62
7	E-1.5-20	77.20
8	E-1.5-30	81.74
9	E-2-10	84.27
10	E-2-20	83.28
11	E-2-30	87.39

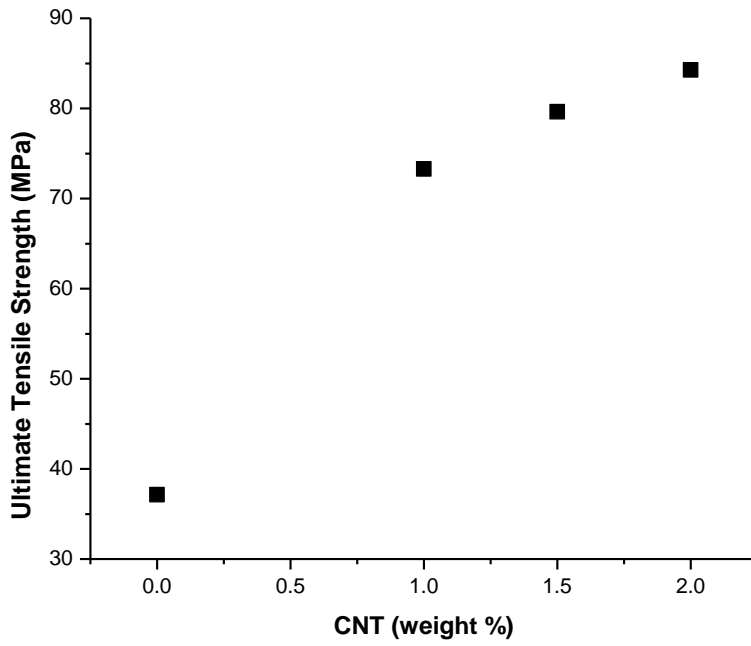


Figure 3.31: Values of ultimate tensile strength against CNT loading.

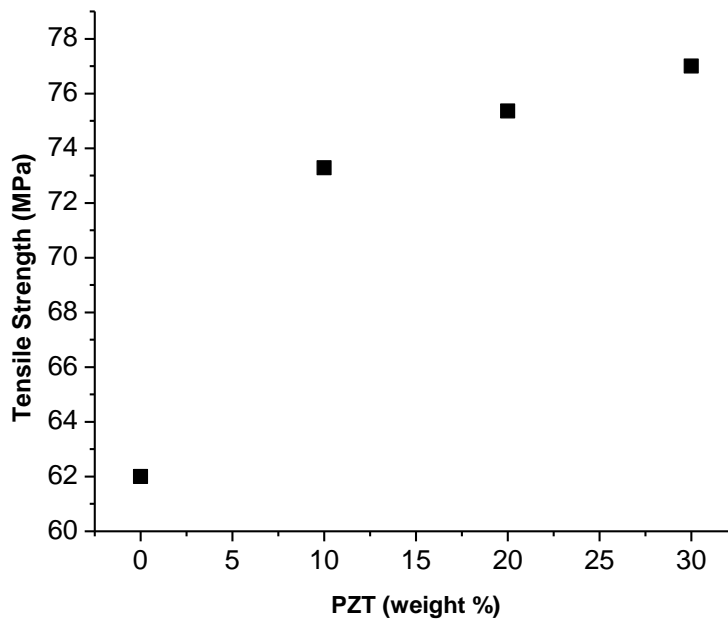


Figure 3.32: Values of ultimate tensile strength against PZT loading.

3.3 Electrical conductivity

Electrical conductivities were calculated by varying the carbon nanotube concentration because carbon nanotubes are responsible for conductive nature of the composites [147]. Electrical conductivity of epoxy is very low and it behaves just like insulator and PZT itself is responsible for insulating nature of the epoxy composites. For piezoelectric composites electrical conductivity plays very important role in their performance. PZT produces electric current in response to mechanical stress and that current when fully disperses in the composite matrix can be stored in the batteries. For piezoelectric performance good dispersion of electric current is necessary. Basically CNTs were used as conductive inclusions to increase the conductive nature of the composites.

Table 3.7 shows the conductivity data for the composites, in Figure 3.33. Electrical conductivity is studied by varying the amount of carbon nanotubes, it is seen from the graph that by increasing the CNT loading in the composites electrical conductivities increases [125, 128]. It is also observed that when CNT percentage is increased from 0.5 to 1.5% there is a sharp increase in conductivities the composites in which 2% CNTs are used shows maximum conductivity values. After 2% more increase in CNTs does not caused remarkable increase in the conductivities as reported by many scientists in literature [129]. Possible reasons for that are CNT agglomerations are formed which reduces the current dispersion and cause decrease in the conductivities of the composites. Another reason is by using CNTs more than 2% in the composite phase separation occurs and carbon nanotubes are not homogenously dispersed in the matrix medium.

PZT is responsible for the insulating nature of the composites as it is shown in table. The composites having equal amount of CNTs, the composites having more PZT shows less conductivity because by increasing amount of PZT electrical conductivity is decreased [148].

Table 3.7: Calculated electrical conductivities for all composites.

S.No.	Sample	Electrical Conductivity (Sm^{-1})
1	E-0-0	1.1301×10^{-7}
2	E-1-0	1.3522×10^{-4}
3	E-1-10	1.5664×10^{-4}
4	E-1-20	1.0870×10^{-4}
5	E-1-30	6.3972×10^{-5}
6	E-1.5-10	2.8765×10^{-4}
7	E-1.5-20	2.0990×10^{-4}
8	E-1.5-30	1.3534×10^{-4}
9	E-2-10	3.4730×10^{-4}
10	E-2-20	2.6315×10^{-4}
11	E-2-30	1.8007×10^{-4}

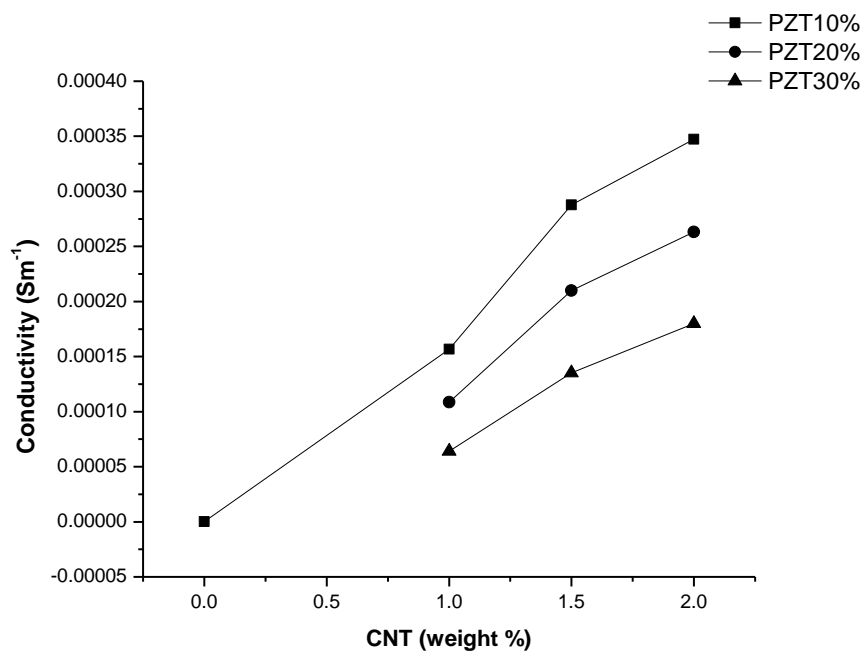


Figure 3.33: Values of electrical conductivities as a function of CNT loading.

3.4 Conclusions

Preparation of piezoelectric composites containing epoxy as a matrix, multiwalled carbon nanotubes (MWCNTs) and lead zirconate titanate (PZT) as reinforcements was done successfully.

XRD analysis proved the amorphous behavior of the cured epoxy while MWCNTs and PZT gave a characteristic sharp peak, which proved crystalline nature of the PZT. XRD of the composite gave information about the fine dispersion of MWCNTs and PZT in the epoxy matrix.

Thermal analysis of the composites was studied by differential scanning calorimetry (DSC). DSC gave the glass transition temperature of all the composites, all the cured samples and the composites showed higher glass transition temperature than neat epoxy. It was observed that increase in weight % of the MWCNTs caused slight decrease in glass transition temperature of the epoxy, while glass transition temperature was found to be increase by increasing the amount of PZT in the matrix.

Thermal degradation of the composites was studied by using thermogravimetric analysis (TGA). TGA was used to study thermal stability of the composites and effect of fillers on the thermal degradation of the epoxy matrix, it was observed that by increasing the weight % of both MWCNTs and PZT maximum degradation temperature shifted to a higher value which proves increased thermal stability of the epoxy matrix by addition of fillers.

Mechanical properties were studied by using tensile testing, various parameters were calculated and effect of MWCNTs and PZT on the mechanical properties of the matrix were checked. It was proved that MWCNTs decrease the brittleness of the epoxy and the composites have less brittleness than the cured epoxy and PZT crystals which enhances its uses and applications. It was proved that by increase in weight % of the MWCNTs toughness, Young's modulus, stress at break and ultimate tensile strength increases. Addition of PZT causes decrease in toughness because PZT itself is a brittle material, by increasing the weight % of the PZT young's modulus, stress at break and ultimate tensile strength increases. Mechanical analysis proved that by using MWCNTs as a reinforcement in epoxy matrix brittleness of the epoxy matrix and PZT decreases which is very useful to overcome the problems associated with limitations of the PZT due to its brittle nature.

References

1. Mallick, P.K., *Composites Engineering Handbook*. 1997: Taylor & Francis.
2. Cha, K.K., *Compos. Sci. Technol.* 2013: Springer New York.
3. Middleton, B., 3 - Composites Part A - *Cherrington, Vanessa GoodshipBethany MiddletonRuth*, in *Design and Manufacture of Plastic Components for Multifunctionality*. 2016, William Andrew Publishing: Oxford. p. 53-101.
4. Heinemann, S., *Chapter 1 - Polymer-Based Matrix Composites A2 - Makhlouf, Abdel Salam Hamdy*, in *Handbook of Nanoceramic and Nanocomposite Coatings and Materials*, D. Scharnweber, Editor. 2015, Butterworth-Heinemann. p. 3-27.
5. Feng, J. and Z. Guo, *Temperature-frequency-dependent mechanical properties model of epoxy resin and its composites*. *Composites Part B*, 2016. **85**: p. 161-169.
6. Fiore, V. and A. Valenza, 5 - *Epoxy resins as a matrix material in advanced fiber-reinforced polymer (FRP) composites A2 - Bai, Jiping*, in *Advanced Fibre-Reinforced Polymer (FRP) Composites for Structural Applications*. 2013, Woodhead Publishing. p. 88-121.
7. Li, M., et al., *Striking effect of epoxy resin on improving mechanical properties of poly(butylene terephthalate)/recycled carbon fibre composites*. *Compos Sci Technol*, 2016. **125**: p. 9-16.
8. Przybytniak, G., et al., *Gamma-rays initiated cationic polymerization of epoxy resins and their carbon nanotubes composites*. *Radiat Phys Chem*, 2016. **121**: p. 16-22.
9. Van Velthem, P., et al., *Phenoxy nanocomposite carriers for delivery of nanofillers in epoxy matrix for resin transfer molding (RTM)-manufactured composites*. *Compos part a-appl s.*, 2015. **76**: p. 82-91.
10. Kandola, B.K., L. Krishnan, and J.R. Ebdon, *Blends of unsaturated polyester and phenolic resins for application as fire-resistant matrices in fibre-reinforced composites: Effects of added flame retardants*. *Polym Degrad Stab*, 2014. **106**: p. 129-137.
11. Miskolczi, N., 3 - *Polyester resins as a matrix material in advanced fibre-reinforced polymer (FRP) composites A2 - Bai, Jiping*, in *Advanced Fibre-*

- Reinforced Polymer (FRP) Composites for Structural Applications*. 2013, Woodhead Publishing. p. 44-68.
12. Sarasini, F. and C. Santulli, *4 - Vinylester resins as a matrix material in advanced fibre-reinforced polymer (FRP) composites A2 - Bai, Jiping*, in *Advanced Fibre-Reinforced Polymer (FRP) Composites for Structural Applications*. 2013, Woodhead Publishing. p. 69-87.
 13. Siriruk, A. and D. Penumadu, *Degradation in fatigue behavior of carbon fiber–vinyl ester based composites due to sea environment*. *Composites Part B*, 2014. **61**: p. 94-98.
 14. Zhang, Z., et al., *A strategy and mechanism of fabricating flame retarding glass fiber fabric reinforced vinyl ester composites with simultaneously improved thermal stability, impact and interlaminar shear strengths*. *Polym Degrad Stab*, 2016. **125**: p. 49-58.
 15. Frollini, E., C.G. Silva, and E.C. Ramires, *2 - Phenolic resins as a matrix material in advanced fiber-reinforced polymer (FRP) composites A2 - Bai, Jiping*, in *Advanced Fibre-Reinforced Polymer (FRP) Composites for Structural Applications*. 2013, Woodhead Publishing. p. 7-43.
 16. Kandola, B.K., et al., *Blends of unsaturated polyester and phenolic resins for application as fire-resistant matrices in fibre-reinforced composites. Part 2: Effects of resin structure, compatibility and composition on fire performance*. *Polym Degrad Stab*, 2015. **113**: p. 154-167.
 17. Si, J., et al., *Enhanced thermal resistance of phenolic resin composites at low loading of graphene oxide*. *Composites Part A*., 2013. **54**: p. 166-172.
 18. Li, S., et al., *Study on thermal conductive BN/novolac resin composites*. *Thermochim Acta*, 2011. **523**(1–2): p. 111-115.
 19. Faghihi, M., A. Shojaei, and R. Bagheri, *Characterization of polyamide 6/carbon nanotube composites prepared by melt mixing-effect of matrix molecular weight and structure*. *Composites Part B*: 2015. **78**: p. 50-64.
 20. Mancic, L., et al., *Thermal and mechanical properties of polyamide 11 based composites reinforced with surface modified titanate nanotubes*. *Mater Des*, 2015. **83**: p. 459-467.
 21. Sato, K., A. Ijuin, and Y. Hotta, *Thermal conductivity enhancement of alumina/polyamide composites via interfacial modification*. *Ceram Int*, 2015. **41**(8): p. 10314-10318.

22. Faruk, O., et al., 6 - *Lignin Reinforcement in Thermoplastic Composites*, in *Lignin in Polymer Composites*. 2016, William Andrew Publishing. p. 95-118.
23. Guedes, J., W.M. Florentino, and D.R. Mulinari, *Chapter 4 - Thermoplastics Polymers Reinforced with Natural Fibers A2 - Chandrasekharakurup, Sabu Thomas Robert Shanks Sarathchandran*, in *Design and Applications of Nanostructured Polymer Blends and Nanocomposite Systems*. 2016, William Andrew Publishing: Boston. p. 55-73.
24. Leal, A.A., et al., *Novel approach for the development of ultra-light, fully-thermoplastic composites*. *Mater Des*, 2016. **93**: p. 334-342.
25. Brunner, A.J., 8 - *Fracture mechanics characterization of polymer composites for aerospace applications A2 - Irving, P.E*, in *Polymer Composites in the Aerospace Industry*, C. Soutis, Editor. 2015, Woodhead Publishing. p. 191-230.
26. Al-Oqla, F.M. and S.M. Sapuan, *Natural fiber reinforced polymer composites in industrial applications: feasibility of date palm fibers for sustainable automotive industry*. *J Clean Pr*, 2014. **66**: p. 347-354.
27. Zare, Y. and I. Shabani, *Polymer/metal nanocomposites for biomedical applications*. *Mater Sci Eng, C: C*, 2016. **60**: p. 195-203.
28. Lee, H. and K. Neville, *Handbook of Epoxy Resins*. 1982: Mac Graw-Hill.
29. Chruściel, J.J. and E. Leśniak, *Modification of epoxy resins with functional silanes, polysiloxanes, silsesquioxanes, silica and silicates*. *Prog Polym Sci*, 2015. **41**: p. 67-121.
30. Sun, D. and Y. Yao, *Synthesis of three novel phosphorus-containing flame retardants and their application in epoxy resins*. *Polym Degrad Stab*, 2011. **96**(10): p. 1720-1724.
31. Jeyranpour, F., G. Alahyarizadeh, and B. Arab, *Comparative investigation of thermal and mechanical properties of cross-linked epoxy polymers with different curing agents by molecular dynamics simulation*. *J Mol Graphics Modell*, 2015. **62**: p. 157-164.
32. Rahul, R. and R. Kitey, *Effect of cross-linking on dynamic mechanical and fracture behavior of epoxy variants*. *Composites Part B*, 2016. **85**: p. 336-342.
33. Ferdosian, F., M. Ebrahimi, and A. Jannesari, *Curing kinetics of solid epoxy/DDM/nanoclay: Isoconversional models versus fitting model*. *Thermochim Acta*, 2013. **568**: p. 67-73.

34. Ferdosian, F., et al., *Sustainable lignin-based epoxy resins cured with aromatic and aliphatic amine curing agents: Curing kinetics and thermal properties*. *Thermochim Acta*, 2015. **618**: p. 48-55.
35. Saldivar-Guerra, E. and E. Vivaldo-Lima, *Handbook of Polymer Synthesis, Characterization, and Processing*. 2013: Wiley.
36. Fernández-Francos, X. and X. Ramis, *Structural analysis of the curing of epoxy thermosets crosslinked with hyperbranched poly(ethyleneimine)s*. *Eur Polym J*, 2015. **70**: p. 286-305.
37. Javdanitehran, M., et al., *An iterative approach for isothermal curing kinetics modelling of an epoxy resin system*. *Thermochim Acta*, 2016. **623**: p. 72-79.
38. Flory, P.J., *Principles of Polymer Chemistry*. 1953: Cornell University Press.
39. Ren, R., et al., *Isothermal curing kinetics and mechanism of DGEBA epoxy resin with phthalide-containing aromatic diamine*. *Thermochim Acta*, 2016. **623**: p. 15-21.
40. Fink, J.K., *Chapter 3 - Epoxy Resins*, in *Reactive Polymers Fundamentals and Applications (Second Edition)*. 2013, William Andrew Publishing: Oxford. p. 95-153.
41. Zheng, X., et al., *Thermal properties and non-isothermal curing kinetics of carbon nanotubes/ionic liquid/epoxy resin systems*. *Thermochim Acta*, 2015. **618**: p. 18-25.
42. Chen, L., et al., *Thermal properties of epoxy resin based thermal interfacial materials by filling Ag nanoparticle-decorated graphene nanosheets*. *Compos Sci Technol*, 2016. **125**: p. 17-21.
43. Xiong, X., et al., *The curing kinetics and thermal properties of epoxy resins cured by aromatic diamine with hetero-cyclic side chain structure*. *Thermochim Acta*, 2014. **595**: p. 22-27.
44. Iijima, S., *Helical microtubules of graphitic carbon*. *Nature*, 1991. **354**(6348): p. 56-58.
45. Choudhary, V. and A. Gupta, *Polymer/Carbon Nanotube Nanocomposites*. *Carbon Nanotubes - Polym Ncompo*. 2011.
46. Zhao, C., et al., *Synthesis and characterization of multi-walled carbon nanotubes reinforced polyamide 6 via in situ polymerization*. *Polymer*, 2005. **46**(14): p. 5125-5132.

47. Cai, H., F. Yan, and Q. Xue, *Investigation of tribological properties of polyimide/carbon nanotube nanocomposites* Mater Sci Eng, A.: A, 2004. **364**(1–2): p. 94-100.
48. Noh, Y.J., et al., *Enhanced dispersion for electrical percolation behavior of multi-walled carbon nanotubes in polymer nanocomposites using simple powder mixing and in situ polymerization with surface treatment of the fillers*. Compos Sci Technol, 2013. **89**: p. 29-37.
49. Yazdani, H., B.E. Smith, and K. Hatami, *Multi-walled carbon nanotube-filled polyvinyl chloride composites: Influence of processing method on dispersion quality, electrical conductivity and mechanical properties*. Composites Part A, 2016. **82**: p. 65-77.
50. Liao, Y.-H., et al., *Investigation of the dispersion process of SWNTs/SC-15 epoxy resin nanocomposites*. Mater Sci Eng, A, 2004. **385**(1–2): p. 175-181.
51. Koerner, H., et al., *Deformation–morphology correlations in electrically conductive carbon nanotube—thermoplastic polyurethane nanocomposites*. Polymer, 2005. **46**(12): p. 4405-4420.
52. Kuan, H.-C., et al., *Synthesis, thermal, mechanical and rheological properties of multiwall carbon nanotube/waterborne polyurethane nanocomposite*. Compos Sci Technol, 2005. **65**(11–12): p. 1703-1710.
53. Seo, M.-K. and S.-J. Park, *Electrical resistivity and rheological behaviors of carbon nanotubes-filled polypropylene composites*. Chem Phys Lett, 2004. **395**(1–3): p. 44-48.
54. Seo, M.-K., J.-R. Lee, and S.-J. Park, *Crystallization kinetics and interfacial behaviors of polypropylene composites reinforced with multi-walled carbon nanotubes*. Mater Sci Eng A, 2005. **404**(1–2): p. 79-84.
55. Liao, C.Z., et al., *Novel polypropylene biocomposites reinforced with carbon nanotubes and hydroxyapatite nanorods for bone replacements*. Mater Sci Eng, C, 2013. **33**(3): p. 1380-1388.
56. Kharitonov, A.P., et al., *Reinforcement of bulk ultrahigh molecular weight polyethylene by fluorinated carbon nanotubes insertion followed by hot pressing and orientation stretching*. Compos Sci Technol, 2015. **120**: p. 26-31.
57. Miao, W., et al., *Epitaxial crystallization of precisely fluorine substituted polyethylene induced by carbon nanotube and reduced graphene oxide*. Polymer, 2016. **83**: p. 205-213.

58. Yang, Z., et al., *Fabrication and characterization of poly(vinyl alcohol)/carbon nanotube melt-spinning composites fiber*. Prog Nat Sci, 2015. **25**(5): p. 437-444.
59. Cohen, E., et al., *Evidences for π -interactions between pyridine modified copolymer and carbon nanotubes and its role as a compatibilizer in poly(methyl methacrylate) composites*. Compos Sci Technol, 2013. **79**: p. 133-139.
60. Gao, X., A.I. Isayev, and C. Yi, *Ultrasonic treatment of polycarbonate/carbon nanotubes composites*. Polymer, 2016. **84**: p. 209-222.
61. Sinha Ray, S. and M. Okamoto, *Polymer/layered silicate nanocomposites: a review from preparation to processing*. Prog Polym Sci, 2003. **28**(11): p. 1539-1641.
62. Wang, L., et al., *The relationship between microstructure and mechanical properties of carbon nanotubes/polylactic acid nanocomposites prepared by twin-screw extrusion*. Composites Part A.
63. Yoon, S.-B., E.-H. Yoon, and K.-B. Kim, *Electrochemical properties of leucoemeraldine, emeraldine, and pernigraniline forms of polyaniline/multi-wall carbon nanotube nanocomposites for supercapacitor applications*. J Power Sources, 2011. **196**(24): p. 10791-10797.
64. Gemeiner, P., et al., *Polypyrrole-coated multi-walled carbon nanotubes for the simple preparation of counter electrodes in dye-sensitized solar cells*. Synth Met, 2015. **210, Part B**: p. 323-331.
65. Song, H., et al., *Influence of polymerization method on the thermoelectric properties of multi-walled carbon nanotubes/polypyrrole composites*. Synth Met, 2016. **211**: p. 58-65.
66. Zhu, Y., K. Shi, and I. Zhitomirsky, *Polypyrrole coated carbon nanotubes for supercapacitor devices with enhanced electrochemical performance*. J Power Sources, 2014. **268**: p. 233-239.
67. Lu, X., et al., *Macroporous Carbon/Nitrogen-doped Carbon Nanotubes/Polyaniline Nanocomposites and Their Application in Supercapacitors*. Electrochim Acta, 2016. **189**: p. 158-165.
68. Rong, R., et al., *Facile preparation of homogeneous and length controllable halloysite nanotubes by ultrasonic scission and uniform viscosity centrifugation*. Chem Eng J.

69. Martı, et al., *Sensitivity of single wall carbon nanotubes to oxidative processing: structural modification, intercalation and functionalisation*. Carbon, 2003. **41**(12): p. 2247-2256.
70. Zhang, X., et al., *Sonochemical synthesis of hollow Pt alloy nanostructures on carbon nanotubes with enhanced electrocatalytic activity for methanol oxidation reaction*. Int J Hydrogen Energy, 2015. **40**(41): p. 14416-14420.
71. Chen, W., X. Tao, and Y. Liu, *Carbon nanotube-reinforced polyurethane composite fibers*. Compos Sci Technol, 2006. **66**(15): p. 3029-3034.
72. Liang, G.D. and S.C. Tjong, *Manufacturing and Electrical Properties of Carbon Nanotube Reinforced Polymer Composites A2 - Fakirov, Debes BhattacharyyaStoyko*, in *Synthetic Polymer–Polymer Composites*. 2012, Hanser. p. 193-224.
73. Zhou, H.W., et al., *Carbon fiber/carbon nanotube reinforced hierarchical composites: Effect of CNT distribution on shearing strength*. Composites Part B, 2016. **88**: p. 201-211.
74. Ajayan, P.M., L.S. Schadler, and P.V. Braun, *Nanocomposite Science and Technology*. 2006: Wiley.
75. Sandler, J., et al., *Development of a dispersion process for carbon nanotubes in an epoxy matrix and the resulting electrical properties*. Polymer, 1999. **40**(21): p. 5967-5971.
76. Sandler, J.K.W., et al., *Ultra-low electrical percolation threshold in carbon-nanotube-epoxy composites*. Polymer, 2003. **44**(19): p. 5893-5899.
77. Schwarz, M.-K., W. Bauhofer, and K. Schulte, *Alternating electric field induced agglomeration of carbon black filled resins*. Polymer, 2002. **43**(10): p. 3079-3082.
78. Zhang, D., et al., *Surfactant-assisted reflux synthesis, characterization and formation mechanism of carbon nanotube/europium hydroxide core–shell nanowires*. Appl Surf Sci, 2009. **255**(19): p. 8270-8275.
79. Park, J.-M., et al., *Nondestructive damage sensitivity and reinforcing effect of carbon nanotube/epoxy composites using electro-micromechanical technique*. Mater Sci Eng C, 2003. **23**(6–8): p. 971-975.
80. Wong, M., et al., *Physical interactions at carbon nanotube-polymer interface*. Polymer, 2003. **44**(25): p. 7757-7764.

81. Park, S.-J., H.-J. Jeong, and C. Nah, *A study of oxyfluorination of multi-walled carbon nanotubes on mechanical interfacial properties of epoxy matrix nanocomposites*. Mater Sci Eng A, 2004. **385**(1–2): p. 13-16.
82. Pumera, M., A. Merkoçi, and S. Alegret, *Carbon nanotube-epoxy composites for electrochemical sensing*. Sens Actuators B: Chemical, 2006. **113**(2): p. 617-622.
83. Cui, S., et al., *Characterization of multiwall carbon nanotubes and influence of surfactant in the nanocomposite processing*. Carbon, 2003. **41**(4): p. 797-809.
84. Martin, C.A., et al., *Formation of percolating networks in multi-wall carbon-nanotube–epoxy composites*. Compos Sci Technol, 2004. **64**(15): p. 2309-2316.
85. Moisala, A., et al., *Thermal and electrical conductivity of single- and multi-walled carbon nanotube-epoxy composites*. Compos Sci Technol, 2006. **66**(10): p. 1285-1288.
86. Su, J., L.-L. Ke, and Y.-S. Wang, *Two-dimensional fretting contact analysis of piezoelectric materials*. Int J Solids and Struct, 2015. **73–74**: p. 41-54.
87. Yu, T., et al., *Interfacial dynamic impermeable cracks analysis in dissimilar piezoelectric materials under coupled electromechanical loading with the extended finite element method*. Int J Solids and Struct, 2015. **67–68**: p. 205-218.
88. Zhao, M., et al., *Effects of electrostatic tractions on the interfacial fracture behavior of two-phase piezoelectric materials*. Eng Fract Mech, 2016. **153**: p. 289-301.
89. Dobrynin, A.V. and M. Rubinstein, *Theory of polyelectrolytes in solutions and at surfaces*. Prog Polym Sci, 2005. **30**(11): p. 1049-1118.
90. Giurgiutiu, V., *Chapter 6 - Piezoelectric Wafer Active Sensors*, in *Structural Health Monitoring of Aerospace Composites*. 2016, Academic Press: Oxford. p. 177-248.
91. Xin, Y., et al., *Full-fiber piezoelectric sensor by straight PVDF/nanoclay nanofibers*. Mater Lett, 2016. **164**: p. 136-139.
92. Yoshida, S., et al., *Fabrication and characterization of large figure-of-merit epitaxial PMnN-PZT/Si transducer for piezoelectric MEMS sensors*. Sens Actuators A, 2016. **239**: p. 201-208.
93. Butcher, M., et al., *An experimental evaluation of the fully coupled hysteretic electro-mechanical behaviour of piezoelectric actuators*. Physica B: Condensed Matter.

94. Molter, A., J.S.O. Fonseca, and L.d.S. Fernandez, *Simultaneous topology optimization of structure and piezoelectric actuators distribution*. Appl Math Model.
95. Romasanta, L.J., M.A. Lopez-Manchado, and R. Verdejo, *Increasing the performance of dielectric elastomer actuators: A review from the materials perspective*. Prog Polym Sci, 2015. **51**: p. 188-211.
96. Shin, D.-J., et al., *Multi-layered piezoelectric energy harvesters based on PZT ceramic actuators*. Ceram Int, 2015. **41, Supplement 1**: p. S686-S690.
97. Zhong, S. and Q. Zhang, *Enhanced optical coherence vibration tomography for subnanoscale-displacement-resolution calibration of piezoelectric actuators*. Sens Actuators A, 2015. **233**: p. 42-46.
98. Zhu, F., Z.-h. Qian, and B. Wang, *Wave propagation in piezoelectric layered structures of film bulk acoustic resonators*. Ultrasonics.
99. DeAngelis, D.A. and G.W. Schulze, *Performance of PIN-PMN-PT Single Crystal Piezoelectric versus PZT8 Piezoceramic Materials in Ultrasonic Transducers*. Physics Procedia, 2015. **63**: p. 21-27.
100. Pardo, L., *5 - Piezoelectric ceramic materials for power ultrasonic transducers A2 - Gallego-Juárez, Juan A*, in *Power Ultrasonics*, K.F. Graff, Editor. 2015, Woodhead Publishing: Oxford. p. 101-125.
101. Zhang, H., et al., *A new automatic resonance frequency tracking method for piezoelectric ultrasonic transducers used in thermosonic wire bonding*. Sensors and Actuators A, 2015. **235**: p. 140-150.
102. Shodja, H.M., S.M. Tabatabaei, and M.T. Kamali, *A piezoelectric medium containing a cylindrical inhomogeneity: Role of electric capacitors and mechanical imperfections*. Int J Solids Struct, 2007. **44**(20): p. 6361-6381.
103. Vasta, G., T.J. Jackson, and E. Tarte, *Electrical properties of BaTiO₃ based ferroelectric capacitors grown on oxide sacrificial layers for micro-cantilevers applications*. Thin Solid Films, 2012. **520**(7): p. 3071-3078.
104. Le, M.Q., et al., *Review on energy harvesting for structural health monitoring in aeronautical applications*. Prog Aersp Sci, 2015. **79**: p. 147-157.
105. M'boungui, G., et al., *A hybrid piezoelectric micro-power generator for use in low power applications*. Renew Sust Energ Rev, 2015. **49**: p. 1136-1144.

106. Manrique-Juárez, M.D., et al., *Switchable molecule-based materials for micro- and nanoscale actuating applications: Achievements and prospects*. *Coord Chem Rev*, 2016. **308**, Part 2: p. 395-408.
107. Nadal, C., et al., *Modelling of a beam excited by piezoelectric actuators in view of tactile applications*. *Math Comput Simulat*.
108. Ribeiro, C., et al., *Piezoelectric polymers as biomaterials for tissue engineering applications*. *Colloids and Surfaces B*, 2015. **136**: p. 46-55.
109. Soliman, N.A., et al., *Piezoelectric ring actuator technique to monitor early-age properties of cement-based materials*. *Cem Concr Compos*, 2015. **63**: p. 84-95.
110. Tang, H., et al., *High-Curie-temperature relaxor piezoelectric single crystals for 1.5D ultrasound phased-array applications*. *Mater Lett*, 2015. **145**: p. 258-260.
111. Uchino, K., *1 - The development of piezoelectric materials and the new perspective*, in *Advanced Piezoelectric Materials*. 2010, Woodhead Publishing. p. 1-85.
112. Wang, B.L. and X.H. Zhang, *An electrical field based non-linear model in the fracture of piezoelectric ceramics*. *Int J Solids Struct*, 2004. **41**(16-17): p. 4337-4347.
113. Zhang, T.-Y., M. Zhao, and P. Tong, *Fracture of piezoelectric ceramics*, in *Advances in Applied Mechanics*, G. Erik van der and Y.W. Theodore, Editors. 2002, Elsevier. p. 147-289.
114. Banerjee, S. and K.A. Cook-Chennault, *An investigation into the influence of electrically conductive particle size on electromechanical coupling and effective dielectric strain coefficients in three phase composite piezoelectric polymers*. *Composites Part A*, 2012. **43**(9): p. 1612-1619.
115. Safari, A., B. Jadidian, and E.K. Akdogan, *5.25 - Piezoelectric Composites for Transducer Applications A2 - Zweben*, Anthony KellyCarl, in *Comprehensive Composite Materials*. 2000, Pergamon: Oxford. p. 533-561.
116. Rianyoi, R., et al., *Influence of barium titanate content and particle size on electromechanical coupling coefficient of lead-free piezoelectric ceramic-Portland cement composites*. *Ceram Int*, 2013. 39, Supplement 1: p. S47-S51.
117. Wang, F., et al., *High quality barium titanate nanofibers for flexible piezoelectric device applications*. *Sens Actuators A*, 2015. **233**: p. 195-201.
118. Wang, J.C., et al., *Different piezoelectric grain size effects in BaTiO₃ ceramics*. *Ceram Int*, 2015. **41**(10, Part B): p. 14165-14171.

119. Zhang, Y., et al., *Aligned porous barium titanate/hydroxyapatite composites with high piezoelectric coefficients for bone tissue engineering*. Mater Sci Eng C, 2014. **39**: p. 143-149.
120. Luo, C., G.Z. Cao, and I.Y. Shen, *Development of a lead-zirconate-titanate (PZT) thin-film microactuator probe for intracochlear applications*. Sens Actuators A, 2013. **201**: p. 1-9.
121. Zhang, Y., et al., *Composition design, phase transitions and electrical properties of Sr²⁺-substituted xPZN–0.1PNN–(0.9–x)PZT piezoelectric ceramics*. Ceram Int, 2016. **42**(3): p. 4080-4089.
122. Kuo, D.-H., et al., *Dielectric behaviours of multi-doped BaTiO₃/epoxy composites*. J Eur Ceram Soc, 2001. **21**(9): p. 1171-1177.
123. Blanas, P. and K. Das-Gupta, *Composite Piezoelectric Materials for Health Monitoring of Composite Structures*. MRS Online Proceedings Library Archive, 1999. **604**: p. null-null.
124. Bao, W.S., et al., *A novel approach to predict the electrical conductivity of multifunctional nanocomposites*. Mech Mater, 2012. **46**: p. 129-138.
125. Tian, S., F. Cui, and X. Wang, *New type of piezo-damping epoxy-matrix composites with multi-walled carbon nanotubes and lead zirconate titanate*. Mater Lett, 2008. **62**(23): p. 3859-3861.
126. Barone, C., et al., *Low-frequency electric noise spectroscopy in different polymer/carbon nanotubes composites*. Diamond Relat Mater, 2016. **65**: p. 32-36.
127. Poh, C.L., et al., *Dielectric properties of surface treated multi-walled carbon nanotube/epoxy thin film composites*. Composites Part B 2016. **85**: p. 50-58.
128. Ma, M. and X. Wang, *Preparation, microstructure and properties of epoxy-based composites containing carbon nanotubes and PMN-PZT piezoceramics as rigid piezo-damping materials*. Mater Chem Phys, 2009. **116**(1): p. 191-197.
129. Tian, S. and X. Wang, *Fabrication and performances of epoxy/multi-walled carbon nanotubes/piezoelectric ceramic composites as rigid piezo-damping materials*. J Mater Sci, 2008. **43**(14): p. 4979-4987.
130. Ladani, R.B., et al., *Multifunctional properties of epoxy nanocomposites reinforced by aligned nanoscale carbon*. Mater Des, 2016. **94**: p. 554-564.
131. Hou, P.-X., C. Liu, and H.-M. Cheng, *Purification of carbon nanotubes*. Carbon, 2008. **46**(15): p. 2003-2025.

132. Hou, P.X., et al., *Multi-step purification of carbon nanotubes*. Carbon, 2002. **40**(1): p. 81-85.
133. Yu, W., et al., *Enhanced thermal conductive property of epoxy composites by low mass fraction of organic-inorganic multilayer covalently grafted carbon nanotubes*. Compos Sci Technol.
134. Xu, J., et al., *Enhanced piezoelectric properties of PZT ceramics prepared by direct coagulation casting via high valence counterions (DCC–HVCI)*. Ceram Int, 2016. **42**(2, Part A): p. 2821-2828.
135. Zhang, J., et al., *Investigation of curing kinetics of sodium carboxymethyl cellulose/epoxy resin system by differential scanning calorimetry*. Thermochim Acta, 2012. **549**: p. 63-68.
136. Zhang, Q., et al., *Dispersion stability of functionalized MWCNT in the epoxy–amine system and its effects on mechanical and interfacial properties of carbon fiber composites*. Mater Des, 2016. **94**: p. 392-402.
137. Schilde, C., et al., *Thermal, mechanical and electrical properties of highly loaded CNT-epoxy composites – A model for the electric conductivity*. Compos Sci Technol, 2015. **117**: p. 183-190.
138. Robinson, T., et al., *Sample preparation for thermo-gravimetric determination and thermo-gravimetric characterization of refuse derived fuel*. Waste Manage (Oxford), 2016. **48**: p. 265-274.
139. Hong, S.-k., et al., *Enhanced thermal and mechanical properties of carbon nanotube composites through the use of functionalized CNT-reactive polymer linkages and three-roll milling*. Composites Part A, 2015. **77**: p. 142-146.
140. Wen, J. and G.L. Wilkes, *Organic/Inorganic Hybrid Network Materials by the Sol–Gel Approach*. Chem Mater, 1996. **8**(8): p. 1667-1681.
141. Ma, C., et al., *Fracture resistance, thermal and electrical properties of epoxy composites containing aligned carbon nanotubes by low magnetic field*. Compos Sci Technol, 2015. **114**: p. 126-135.
142. Wang, J., et al., *Microstructure, electrical and mechanical properties of MgO nanoparticles-reinforced porous PZT 95/5 ferroelectric ceramics*. Ceram Int, 2013. **39**(4): p. 3915-3919.
143. Pan, J., et al., *A new micromechanics model and effective elastic modulus of nanotube reinforced composites*. Comput Mater Sci, 2016. **113**: p. 21-26.

144. Liu, P., et al., *Advanced multifunctional properties of aligned carbon nanotube-epoxy thin film composites*. Mater Des, 2015. **87**: p. 600-605.
145. Babu, I. and G. de With, *Highly flexible piezoelectric 0–3 PZT–PDMS composites with high filler content*. Compos Sci Technol, 2014. **91**: p. 91-97.
146. Irshidat, M.R., M.H. Al-Saleh, and M. Al-Shoubaki, *Using carbon nanotubes to improve strengthening efficiency of carbon fiber/epoxy composites confined RC columns*. Compos Struct, 2015. **134**: p. 523-532.
147. Spitalsky, Z., et al., *Carbon nanotube–polymer composites: Chemistry, processing, mechanical and electrical properties*. Prog Polym Sci, 2010. **35**(3): p. 357-401.
148. Pascariu, V., et al., *Dielectric properties of PZT–epoxy composite thick films*. J Alloys Compd, 2013. **574**: p. 591-599.